Table 4
Selected spots by SGB

(A) HCC

ID	SGB variable importance	Decyder		Protein name
		Ratio[a]	p-value (t-test)	
1977	30.66595	0.36	<1.0E−17	Carbonic anhydrase 2
560	29.66868	2.17	2.20E−13	Heat shock protein 90 kDa alpha
789	23.52533	1.84	2.20E−16	Annexin A6
1699	9.47421	6.98	<1.0E−17	Aldo-keto reductase family 1, member B10
366	3.07334	1.76	<1.0E−17	Heat shock 70 kDa protein 4
718	1.87712	2.12	5.70E−09	Heat shock 70 kDa protein 5
2012	0.71447	0.55	<1.0E−17	Enoyl Coenzyme A hydratase, short chain, 1
564	0.37075	1.37	0.0003	Transferrin
1007	0.15318	1.61	3.10E−07	Protein disulfide isomerase-associated 3
1556	0.12636	0.67	6.70E−10	Aldo-keto reductase 1A1
782	0.11134	1.7	1.40E−12	Heat shock 70 kDa protein 8
1331	0.05304	0.47	2.70E−13	Argininosuccinate synthetase
1312	0.05231	0.46	1.90E−09	Argininosuccinate synthetase
1046	0.05206	2.16	<1.0E−17	Vimentin
1582	0.04124	0.52	2.60E−11	Fructose-1,6-bisphosphatase 1
753	0.03851	1.79	3.60E−15	Heat shock 70 kDa protein 9B
2412	0.00211	0.54	3.00E−11	Human fatty acid binding protein FABP
444	0.00001	1.57	5.20E−06	Alpha glucosidase 2

(B) Histological grade

ID	SGB variable importance	Decyder		Protein name
		Ratio[b]	p-value (t-test)	
1129	49.9428	1.8	0.06	Keratin 8
1699	22.8444	0.43	2.00E−06	Aldo-keto reductase family 1, member B10
2423	5.616	1.38	0.064	D-dopachrome tautomerase
2126	4.7494	0.64	0.00041	peroxiredoxin 3
1068	4.6065	0.78	0.061	Glutamate dehydrogenase 1
2082	3.9313	0.77	0.0012	Es1 protein isoform 1a
1044	2.3596	0.61	0.068	Aldehyde dehydrogenase 1 family, member A1
999	1.6503	0.81	0.0033	Formiminotransferase cyclodeaminase
2039	1.2688	0.77	0.0088	Rho GDP dissociation inhibitor alpha
1685	1.1069	0.49	1.00E−05	Aldo-keto reductase 1B10
2025	0.6014	0.9	0.55	Heat shock 27 kDa protein 1
1036	0.4462	0.63	0.025	Aldehyde dehydrogenase 1 family, member A1
1059	0.3658	0.73	0.0054	Leucine aminopeptidase 3
1016	0.3094	0.98	0.11	Glucose regulated protein, 58 kDa
1027	0.0579	0.67	0.021	aldehyde dehydrogenase 1A1
1054	0.0558	0.73	0.015	Glutamate dehydrogenase 1
2159	0.0462	0.69	0.00038	Abhydrolase domain containing 14B
235	0.0204	1.13	0.48	Carbamoyl-phosphate synthetase 1
966	0.007	0.75	0.017	UDP-glucose dehydrogenase
2238	0.0044	0.93	0.054	Non-metastatic cells 1 protein
1086	0.003	0.98	0.87	UDP-glucose pyrophosphorylase 2
782	0.0025	1.19	0.25	Heat shock 70 kDa protein 8
2201	0.0018	0.76	0.025	Prostatic binding protein
1842	0.001	0.84	0.11	Electron-transfer-flavoprotein alpha subunit
798	0.0004	0.78	0.0021	Programmed cell death 8
1510	0.0004	0.78	0.0017	Acyl-Coenzyme A dehydrogenase, short/branched chain
1414	0.0001	0.93	0.14	Acetyl-Coenzyme A acetyltransferase 1

(C) AFP level

ID	SGB variable importance	Decyder		Protein name
		Ratio[c]	p-value (t-test)	
798	22.143	0.76	0.0002	Programmed cell death 8
1129	21.8696	1.62	0.25	Keratin 8
1007	12.4499	0.69	0.018	Protein disulfide isomerase-associated 3
1515	10.5222	0.81	0.95	Galactokinase 1
451	10.1806	0.85	0.37	Glucosidase, alpha; neutral AB
2159	7.1303	0.64	0.0065	Abhydrolase domain containing 14B
782	2.8347	1.18	0.0045	Annexin A6
659	2.7554	1.37	0.055	Lamin A/C
808	2.1413	0.7	0.0039	Carnitine palmitoyltransferase 2

Table 4 *(continued)*

(C) AFP level

ID	SGB variable importance	Decyder		Protein name
		Ratio[a]	p-value (t-test)	
1414	1.4418	0.81	0.01	Acetyl-Coenzyme A acetyltransferase 1
2082	1.4242	0.79	0.00028	Es1 protein isoform 1a
1219	1.2098	0.69	0.0083	Enolase 1
2010	1.1381	1.26	0.62	Enoyl-coenzyme A hydratase 1
1376	1.0921	0.61	0.00098	Actin, beta
2347	0.9536	1.35	0.001	Hemoglobin, beta
2364	0.2937	2.28	0.00013	Hemoglobin, beta
1794	0.1273	1.51	0.36	Sulfotransferase family, cytosolic, 2A, dehydroepiandrosterone-preferring, member 1
1383	0.0946	1.16	0.034	Aminoacylase 1
2423	0.0842	0.99	0.2	D-dopachrome tautomerase
1145	0.0647	0.95	0.058	ATP synthase, H+ transporting, mitochondrial F1 complex, beta polypeptide
1889	0.0281	1.12	0.41	Ketohexokinase
1795	0.0131	1.33	0.95	Sulfotransferase family, cytosolic, 2A, dehydroepiandrosterone (DHEA) -preferring, member 1
235	0.0045	0.87	0.063	Carbamoyl-phosphate synthetase 1, mitochondrial
1551	0.0028	1.35	0.7	Arginase 1
2039	0.0003	1.03	0.15	Rho GDP dissociation inhibitor alpha

[a] Ratio represents the average spot volume ratio of HCC/non HCC.
[b] Ratio represents the average spot volume ratio of moderate/well.
[c] Ratio represents the average spot volume ratio of high AFP/low AFP.

and test sets overall. For HCC and histological grade, SGB performs very well. For AFP, the accuracy of test sets is 71.4%. Although the performance of SGB depends on data sets, present results suggest that the spots selected by SGB are discriminative. From Table 4 (A)–(C), one can see that variable importance does not always correspond to p-value of t-test. This difference originates from that variable importance simultaneously incorporates multiple spots to classify the groups as described in Section 2.10, while t-test only incorporates average of each spots. Accordingly, one can detect the informative spots that contribute to sample classification through SGB. These discussions explain that SGB worked well for AFP in spite of the average spot value ratio of almost one.

To visualize the degree of discrimination for each data set by the selected spots, we show the scatter plots by two spots for each class in Fig. 5. One can see that the two spots discriminate each gel better than one spot. Thus, we demonstrated that supervised feature selection surely works well for detection of discriminative and informative proteins. Our results suggest that the SGB is able to detect the spots associated with tissue types using only identified spots.

3.4. Protein spots associated with HCC, histological grade and AFP

From Table 4(A), heat shock proteins (heat shock protein 90 kDa alpha, heat shock 70 kDa protein 4, heat shock 70 kDa protein 5, heat shock 70 kDa protein 8, heat shock 70 kDa protein 9B), protein disulfide isomerase-associated 3 (PDIA3) and aldo-keto reductase 1B10 (AKRB10) were overexpressed in HCC. These events are common at least three members of HSP family (HSP90, HSP70, HSC71) have been reported in prior works [14,28,29]. Members of the heat shock protein family have been known to promote cancer cell growth and survival by distinct mechanism [30]. HSP family were first discovered by their elevated abundance after heat shock. They take part in protein folding processes in normal physiological conditions. They bind and prevent non-native proteins from aggregation. Heat shock 70 kDa protein 5 (GRP78) is a member of HSP70 family localized in endoplasmic reticulum (ER). Expression of GRP78 can be induced in response to different stimuli including glucose starvation, hypoxia and ER

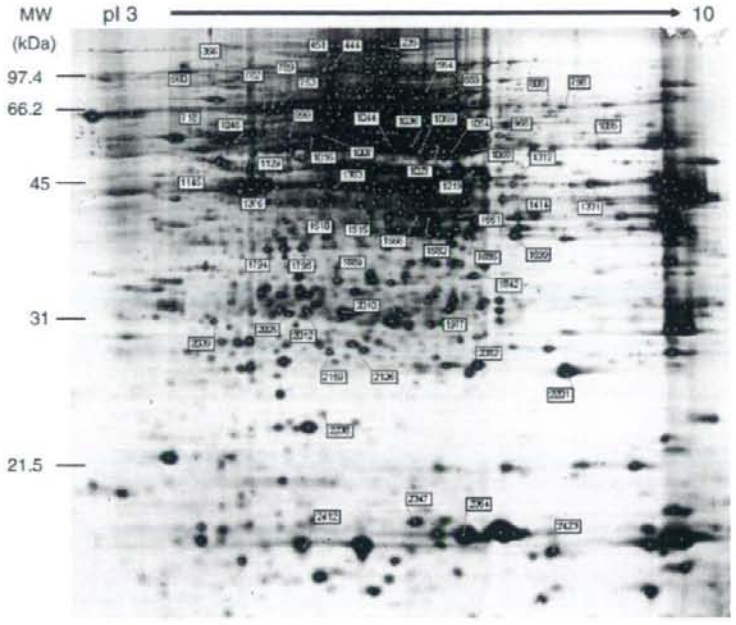

Fig. 4. Representative 2D image of the preparative gel. The gel was post-stained with SYPRO Ruby (Invitrogen). The numbers indicate spots associated with HCC, spots associated with grade and spots associated with AFP.

Ca2+ pool depletion [31]. GRP78 has been proven to protect cells from apoptosis, probably through inhibition of caspase-7 activation, an apoptotic executioner [32]. Highly induced GRP78 in progressively growing tumor cells has been reported to protect them from immune attack, thus preventing tumor regression [33]. High level of GRP78 observed in this study may also support the aggressive growth and the suppression of tumor rejection in HCC. In this study, carbonic anhydrase 2 (CAII) is poorly expressed in HCC, being consistent with the report of Kuo et al. [34] They concluded that this might promote tumor cell motility and contribute to tumor growth and metastasis.

In addition, heat shock 70 kDa protein 9B (mortalin) is abundantly expressed in HCC. Yi et al. [35] recently found that overexpression of mortalin in HCC was associated with HCC metastasis and early recurrence using 2-DE, quantitative PCR, western blot and immunohistochemistry. Poor expression of argininosuccinate synthetase (ASS) is one of well-known molecular features of HCC and is recently a target of HCC treatment using arginine-depleting enzymes [36]. Vimentin (VIM) is abundantly expressed in HCC. Hu et al. [37] reported that overexpression of VIM is significantly associated with HCC metastasis using cDNA microarray and tissue microarray.

Table 5
Performance evaluation for classification

Training sets	
Data sets	Accuracy (%)
HCC/non HCC	100
Moderate/well	100
Low AFP/high AFP	94.1
Test sets	
Data sets	Accuracy (%)
HCC/non HCC	100
Moderate/well	93.3
Low AFP/high AFP	71.4

(a) HCC (HCC/non HCC), (b) histological grade (moderate/well), (c) AFP level (low AFP/high AFP).

Furthermore, we examined gene expression level of selected proteins by RTD-PCR and cDNA microarray (Table S1 (a)). Most of these results are also consistent with protein expression profiles.

Although previous studies dealt with large size HCC or HCC with progressive stage, we dealt with small size HCC in this study. The proteins shown here might be potential biomarkers for early diagnosis.

Table 4 (B) and (C) represent protein spots associated with histological grade in HCC, and protein spots associated with AFP level, respectively. Table 4 (B) shows that several metabolic enzymes, such as AKRB10, glutamate dehydrogenase 1 (GLUD1), aldehyde dehydrogenase 1A1, and peroxiredoxin3 (PRDX3) were poorly expressed in moderate HCC cells, and keratin 8 (KRT8) were abundantly expressed in moderate HCC. It has been reported that the message of AKR1B10 was expressed most abundantly in small intestine and colon, while with lower levels in liver, thymus, prostate, testis, and skeletal muscle in normal tissues [38]. From our results, although AKR1B10 abundantly expressed in HCC compared with non HCC, it poorly expressed in moderate grade compared with well grade. The reason of this could be explained well, however different metabolic process in moderate differentiated HCC might not support the high expression of this gene as found in well differentiated HCC. GLUD1 has been reported poorly expressed in HCC [39]. This may suggest that GLUD1 is related to both HCC and grade. PRDX3 is required for MYC-mediated proliferation, transformation, and apoptosis after glucose withdrawal and essential for maintaining mitochondrial mass and membrane potential in transformed rat and human cells and deregulated expression of the MYC transcription factor is found in a wide variety of human tumors. These data provided evidence that PRDX3 is a MYC target gene that is required to maintain normal mitochondrial function [40].

AFP is the most established tumor marker in HCC and the gold standard by which other markers for the disease are judged [41]. Approximately, 70% of HCC are associated with AFP, and some HCC produce low level of AFP. Although small tumors tend to produce lower levels of AFP, direct relationship between serum AFP and tumor size has not been established as yet. Younger patients and men tend to have higher levels compared to older patients and women, respectively

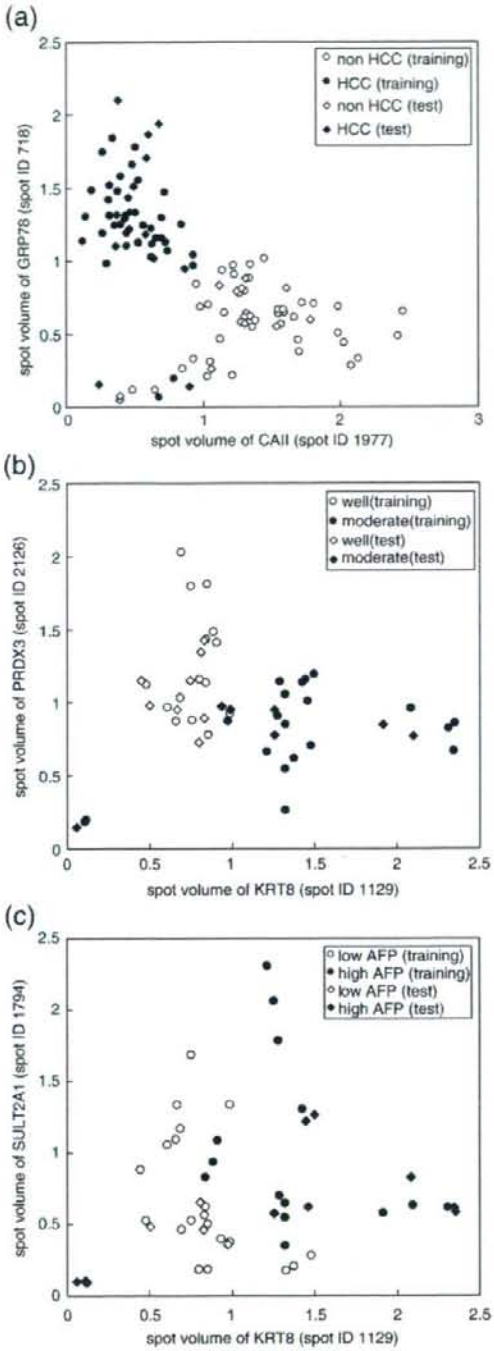

Fig. 5. The scatter plots by two spots. (a) HCC/non HCC, (b) histological grade of moderate/well, (c) high AFP/low AFP level.

[42,43]. From Table 4 (C), two structural protein, KRT8 and lamin A/C were abundantly expressed in HCC cells associated with higher levels of AFP, whereas two apotosis related proteins, programmed cell death 8 and sulfotransferase family, cytosolic, 2A, dehydroepiandrosterone-prefering, member1 (SULT2A1) and PDIA3 were poorly expressed in HCC cells associated with higher levels of AFP.

The overexpression of KRT8 also has been reported by Western blot and immunofluorescence analysis in higher metastatic HCC cell lines [44]. This implies that the alternation of KRT8 in its expression level might be related to metastatic ability. In this study, we observed that KRT8 expressed abundantly in both moderate HCC and high AFP level.

Chignard et al. has reported that a highly significant difference in PDIA3 fragment serum levels among HCC patients, at-risk patients (patients with chronic hepatitis or cirrhosis) and healthy individuals was observed [45]. However, they did not investigate the correlation between HCC and AFP. On the other hand, we observed that PDIA3 was poorly expressed in HCC cells associated with higher levels of AFP. Hence, our results suggest that AFP and PDIA3 may be complementarily expressed abundantly in serum.

Note that the differentially expressed proteins associated with histological grade of HCC and AFP level found in this study, are not always specific for HCC. PDIA3 has been reported to be differentially expressed in brain and breast cancer [46,47]. AKR1B10 has been involved also in lung cancer [48]. Also, it has been known that cytokeratins including KRT8 are part of the epithelial–mesenchymal transition (EMT). EMT is originally an embryonic developmental process that is hijacked by cancer cells in colorectal cancer [49]. However, our finding in this pilot study could provide new insights on understanding the pathogenesis of HCC, histological grade and AFP level.

4. Conclusion

We performed 2D-DIGE combined with MS to analyze the proteomic profiling of HCC and their surrounding non HCC obtained from 18 HCC patients. We identified the discriminative and informative protein spots associated with HCC, histological grade and AFP level using feature selection with SGB. We confirmed that the proposed method is able to identify known HCC-related proteins, e.g., HSP70 family. Moreover, we identified the potential biomarkers associated with histological grade of HCC and AFP level and found that AKR1B10 is related to,well differentiated HCC KRT8 is related to both cell differentiation and AFP level and PDIA3 is associated with both HCC and AFP level. Although the list of selected spots can be changed depending on training sets as pointed by Michiels et .al. [50], we showed that our present results for HCC are consistent with many prior studies and it appears that the obtained results are certainly reliable. Since all HCC samples were stage I, we observed the molecular events of relatively early stage of tumor. Our results shed light on understanding of the pathogenesis mechanism of HCC, histological grade and AFP level and will contribute to therapy and treatments for HCC. Although we only deal with small number of samples in this study, our strategy may be useful for detection of diagnosis or prognosis biomarkers when large number of samples are available.

Acknowledgement

The authors thank to Naoko Tetsura for excellent technical assistance.

Appendix A. Supplementary data

Supplementary data associated with this article can be found, in the online version, at doi:10.1016/j.bbapap.2008.02.011.

References

[1] D.M. Parkin, P. Pisani, J. Ferlay, Global cancer statistics, Cancer J. Clin. 49 (1999) 33–64.
[2] P. Pisani, D.M. Parkin, F. Bray, J. Ferley, Estimates of the world wide mortality from 25 cancers in 1990, Int. J. Cancer 83 (1999) 18–29.
[3] H.B. El-Serag, A.C. Mason, Rising incidence of hepatocelluar carcinoma in the United States, N. Engl. J. Med. 340 (1999) 745–750.

[4] S.D. Taylor-Robinson, G.R. Foster, S. Arora, H.C. Thomas, Increase in primary liver cancer in the UK, Lancet 350 (1997) 1142–1143.
[5] L.J. Lopez, J.A. Marrero, Hepatocellular carcinoma, Curr. Opin. Gastroenterol. 3 (2004) 248–253.
[6] H. Okabe, T. Satoh, T. Kato, O. Kitahara, R. Yanagawa, Y. Yamaoka, T. Tsunoda, Y. Furukawa, Y. Nakamura, Genomewide analysis of gene expression in human hepatocellular carcinomas using cDNA microarray: identification of genes involved in viral carcinogenesis and tumor progression, Cancer Res. 13 (2001) 2129–2137.
[7] X. Chen, S.T. Cheung, S. So, S.T. Fan, C. Barray, J. Higgins, K.M. Lai, J. Ji, S. Dudoit, I.O. Ng, M. Van De Rijn, D. Botstein, P.O. Brown, Gene expression patterns in human liver cancers, Mol. Biol. Cell 13 (2002) 1929–1939.
[8] M.W. Smith, Z.N. Yue, G.K. Geiss, N.Y. Sadovnikova, V.S. Carter, L. Boix, C.A. Lazaro, G.B. Rosenberg, R.E. Bumgarner, N. Fausto, J. Bruix, M.G. Katze, Identification of novel tumor markers in hepatitis C virus-associated hepatocellular carcinoma, Cancer Res. 63 (2003) 859–864.
[9] T. Yamashita, S. Kaneko, T. Hashimoto, S. Sato, N. Nagai, T. Toyoda, K. Suzuki, K. Kobayashi, K. Matsushima, Serial analysis of gene expression in chronic hepatitis C and hepatocellular carcinoma, Biochem. Biophys. Res. Commun. 282 (2001) 647–654.
[10] Q.H. Ye, L.X. Qin, M. Forgues, P. He, J.W. Kim, A.C. Peng, R. Simon, Y. Li, A.I. Robles, Y. Chen, Z.C. Ma, Z.Q. Wu, S. Ye, Y.K. Liu, Z.Y. Tang, X.W. Wang, Predicting hepatitis B virus-positive metastatic hepatocellular carcinoma using gene expression profiling and supervised machine learning, Nat. Med. 9 (2003) 416–423.
[11] P.J. Wirth, T.N. Hoang, T. Benjamin, Micorpreparative immobilized pH gradient two-dimensional electrophoresis in combination with protein microsequencing for the analysis of human liver proteins, Electrophoresis 16 (1995) 1946–1960.
[12] T.K. Seow, S.E. Ong, R.C. Liang, E.C. Ren, L. Chan, K. Ou, M.C. Chung, Two-dimensional electrophoresis map of the human hepatocellular carcinoma cell line, HCC-M, and identification of the separated proteins by mass spectrometry, Electrophoresis 21 (2000) 1787–1813.
[13] K.S. Park, S.Y. Cho, H. Kim, Y.K. Paik, Proteomic alternations of the variants of human aldehyde dehydrogenase isozymes correlate with hepatocellular carcinoma, Int. J. Cancer 97 (2002) 261–265.
[14] S.O. Lim, S.J. Park, W. Kim, S.G. Park, H.J. Kim, Y.I. Kim, T.S. Sohn, J.H. Noh, G. Jung, Proteomic analysis of hepatocellular carcinoma, Biochem. Biophys. Res. Commun. 291 (2002) 1031–1037.
[15] K.S. Park, H. Kim, N.G. Kim, S.Y. Cho, K.H. Choi, J.K. Seong, Y.K. Paik, Proteomic analysis and molecular characterization of tissue ferritin light chain in hepatocellular carcinoma, Hepatology 35 (2002) 1459–1466.
[16] M. Unlu, J.S. Morgan, J.S. Minden, Difference gel electrophoresis: a single gel method for detecting changes in protein extracts, Electrophoresis 11 (1997) 2071–2077.
[17] M.R. Knowles, S. Cervino, H.A. Skynner, S.P. Hunt, C. de Felipe, K. Salim, G. Meneses-Lorente, G. McAllister, P.C. Guest, Multiplex proteomic analysis by two-dimensional differential in gel electrophoresis, Proteomics 3 (2003) 1162–1171.
[18] J. Shaw, R. Rowlinson, J. Nickson, T. Stone, A. Sweet, K. Williams, R. Tonge, Evaluation of saturation labeling two-dimensional difference gel electrophoresis fluorescent dyes, Proteomics 3 (2003) 1181–1195.
[19] G. Van den Bergh, L. Arckens, Fluorescent two-dimensional difference gel electrophoresis unveils the potential of gel-based proteomics, Curr. Opin. Biotechnol. 15 (2004) 38–43.
[20] A. Alban, S.O. David, L. Bjorkesten, C. Anderson, E. Sloge, S. Lewis, I. Currie, A novel experimental design for comparative two-dimensional gel analysis: two-dimensional difference gel electrophoresis incorporating a pooled internal standard, Proteomics 1 (2003) 36–44.
[21] J.H. Friedman, Stochastic gradient boosting, Comput. Stat. Data Anal. 38 (2002) 367–378.
[22] K.G. Ishak, P.P. Anthony, L.H. Sobin, Histological typing Classification of Tumors, Springer-Verlag, New York, 1994.
[23] Minagawa, J., Honda, M., Miyazaki, K., Tabuse, Y., Teramoto, R., Yamashita, T., Nishino, K., Takatori, H., Ueda, T., Kamijo, K., Kaneko, S., Comparative proteomic and transcriptomic profiling of the human hepatocellular carcinoma. Biochem. Biophys. Res. Commun. in press.
[24] M. Honda, T. Yamashita, T. Ueda, R. Takatori, R. Nishino, S. Kaneko, Different signaling pathways in the livers of patients with chronic hepatitis B or chronic hepatitis C, Hepatology 44 (2006) 1122–1138.
[25] O. Troyanskaya, M. Cantor, G. Sherlock, P. Brown, T. Hastei, R. Tibshirani, D. Botstein, R.B. Altman, Missing value estimation methods for DNA microarrays, Bioinformatics 17 (2001) 520–525.
[26] J.H. Friedman, Greedy function approximation: a gradient boosting machine, Ann. Stat. 29 (2001) 1189–1232.
[27] A. Dupuy, R.M. Simon, Critical review of published microarray studies for cancer outcome and guidelines on statistical analysis and reporting, J. Natl. Cancer Inst. 99 (2007) 147–157 (99).
[28] M. Takashima, Y. Kuramitsu, Y. Yokoyama, N. Iizuka, T. Toda, I. Sakaida, K. Okita, M. Oka, K. Nakamura, Proteomic profiling of heat shock protein 70 family members as biomarkers for hepatitis C virus-related hepatocellular carcinoma, Proteomics 3 (2003) 2487–2493.
[29] W. Kim, S. Oe Lim, J.S. Kim, Y.H. Ryu, J.Y. Byeon, H.J. Kim, Y.I. Kim, J.S. Heo, Y.M. Park, G. Jung, Comparison of proteome between hepatitis B virus- and hepatitis C virus-associated hepatocelluar carcinoma, Clin. Cancer Res. 9 (2003) 5493–5500.
[30] M. Rohde, M. Daugaard, M.H. Jensen, K. Helin, J. Nylandsted, M. Jäättelä, Members of the heat-shock protein 70 family promote cancer cell growth by distinct mechanisms, Genes Dev. 19 (2005) 570–582.
[31] H. Miyake, I. Hara, S. Arakawa, S. Kamidono, Stress protein GRP78 prevents apoptosis induced by calcium ionophore, ionomycin, but not by glycosylation inhibitor, tunicamycin, in human prostate cancer cells, J. Cell. Biochem. 77 (2000) 396–408.
[32] R.K. Reddy, C. Mao, P. Baumeister, R.C. Austin, Endoplasmic reticulum chaperone protein GRP78 protects cells from apoptosis induced by topoisomerase inhibitors: role of ATP binding site in suppression of caspase-7 activation, J. Biol. Chem. 278 (2003) 20915–20924.
[33] C. Jamora, G. Dennert, A.S. Lee, Inhibition of tumor progression by suppression of stress protein GRP78/BiP induction in fibrosarcoma B/C10ME, Proc. Natl. Acad. Sci. U. S. A. 93 (1996) 7690–7694.
[34] W.H. Kuo, W.L. Chiang, S.F. Yang, K.T. Yeh, C.M. Yeh, Y.S. Hsieh, S.C. Chu, The differential expression of cytosolic carbonic anhydrase in human hepatocellular carcinoma, Life Sci. 73 (2003) 2211–2223.
[35] Yi, X., Luk, M. J., Lee, P. N., Peng, J., Leng, X., Guan, X., Lau, K. G., Fan, S., Association of mortalin (HSPA9) with liver cancer metastasis and prediction for early tumor recurrence. Mol. Cell. Proteomics. in press.
[36] N.P. Cheng, T. Lam, W. Lam, S. Tsui, W.A. Cheng, W. Lo, Y. Leung, Pegylated recombinant human arginase (rhArg-peg500mw) inhibits the in vitro and in vivo proliferation of human hepatocellular carcinoma through depletion, Cancer Res. 67 (2007) 309–317.
[37] L. Hu, H.S. Lau, C. Tzang, J. Wen, W. Wang, D. Xie, M. Huang, Y. Wang, M. Wu, J. Huang, W. Zeng, J. Sham, M. Yang, X. Guan, Association of vimentin overexpression and hepatocellular carcinoma metastasis, Oncogene 23 (2004) 298–302.
[38] D. Cao, S.T. Fans, S.S.M. Chung, Identification and characterization of a novel human aldose reductase-like gene, J. Biol. Chem. 273 (1998) 11429–11435.
[39] I.N. Lee, C.H. Chen, J.C. Sheu, H.S. Lee, G.T. Huang, C.Y. Yu, F.J. Lu, L.P. Chow, Identification of human hepatocellular carcinoma-related biomarkers by two-dimensional difference gel electrophoresis and mass spectrometry, J. Proteome Res. 4 (2005) 2062–2069.
[40] D.R. Wonsey, K.I. Zeller, C.V. Dang, The c-Myc target gene PRDX3 is required for mitochondrial homeostasis and neoplastic transformation, Proc. Natl. Acad. Sci. U. S. A. 99 (2002) 6649–6654.
[41] J.B. Lopez, Recent developments in the first detection of hepatocellular carcinoma, Clin. Biochem. Rev. 26 (2005) 65–79.
[42] M.C. Kew, Hepatocellular cancer: a century of progress, Clin. Liver Dis. 4 (2000) 257–268.
[43] P.J. Johnson, The role of serum alpha-fetoprotein estimation in the diagnosis and management of hepatocellular carcinoma, Clin. Liver Dis. 5 (2001) 145–160.
[44] Z. Dai, Y.K. Liu, J.F. Cui, H.L. Shen, J. Chen, R.X. Sun, Y. Zhang, X.W. Zhou, P.Y. Yang, Z.Y. Tang, Identification and analysis of altered alpha1,6-fucosylated glycoproteins associated with hepatocellular carcinoma metastasis, Proteomics 6 (2006) 5857–5867.
[45] N. Chignard, S. Shang, H. Wang, J. Marrero, C. Bréchot, S. Hanash, L. Bereretta, Cleavage of endoplasmic reticulum proteins in hepatocellular carcinoma: detection of generated fragments in patient sera, Gastroenterology 130 (2006) 2010–2022.
[46] F. Odreman, M. Vindigni, M.L. Gonzales, B. Niccolini, G. Candiano, B. Zanotti, M. Skrap, S. Pizzolitto, G. Stanta, A. Vindigni, Proteomic studies on low- and high-grade human brain astrocytomas, J. Proteome Res. 4 (2005) 698–708.
[47] K. Gumireddy, F. Sun, A.J. Klein-Szanto, J.M. Gibbins, P.A. Gimotty, A.J. Saunders, P.G. Schultz, Q. Huang, In vivo selection for metastasis promoting genes in the mouse, Proc. Natl. Acad. Sci. U. S. A. 16 (2007) 6696–6701.
[48] S. Fukumoto, N. Yamauchi, H. Moriguchi, Y. Hippo, A. Watanabe, J. Shibahara, H. Taniguchi, S. Ishikawa, H. Ito, S. Yamamoto, H. Iwanari, M. Hironaka, Y. Ishikawa, T. Niki, Y. Sohara, T. Kodama, M. Nishimura, M. Fukayama, H. Dosaka-Akita, H. Aburatani, Overexpression of the aldo-keto reductase family protein AKR1B10 is highly correlated with smokers' non-small cell lung carcinomas, Clin. Cancer Res. 5 (2005) 1776–1785.
[49] T. Knösel, V. Emde, K. Schlüns, P.M. Schlag, M. Dietel, I. Petersen, Cytokeratin profiles identify diagnostic signatures in colorectal cancer using multiplex analysis of tissue microarrays, Cell. Oncol. 28 (2006) 167–175.
[50] S. Michiels, S. Koscielny, C. Hill, Prediction of cancer outcome with microarrays: a multiple random validation strategy, Lancet 365 (2005) 488–492.

Available online at www.sciencedirect.com
ScienceDirect
Biochemical and Biophysical Research Communications 366 (2008) 186–192
BBRC
www.elsevier.com/locate/ybbrc

Comparative proteomic and transcriptomic profiling of the human hepatocellular carcinoma

Hirotaka Minagawa [a], Masao Honda [b,*], Kenji Miyazaki [c], Yo Tabuse [c,*], Reiji Teramoto [c], Taro Yamashita [b], Ryuhei Nishino [b], Hajime Takatori [b], Teruyuki Ueda [b], Ken'ichi Kamijo [a], Shuichi Kaneko [b]

[a] *Nano Electronics Research Laboratories, NEC Corporation, 34, Miyukigaoka, Tsukuba, Ibaraki 305-8501, Japan*
[b] *Department of Gastroenterology, Kanazawa University Graduate School of Medical Science, Kanazawa, 13-1 Takara-machi, Kanazawa 920-8641, Japan*
[c] *Bio-IT Center, NEC Corporation, 34, Miyukigaoka, Tsukuba, Ibaraki 305-8501, Japan*

Received 14 November 2007
Available online 4 December 2007

Abstract

Proteome analysis of human hepatocellular carcinoma (HCC) was done using two-dimensional difference gel electrophoresis. To gain an understanding of the molecular events accompanying HCC development, we compared the protein expression profiles of HCC and non-HCC tissue from 14 patients to the mRNA expression profiles of the same samples made from a cDNA microarray. A total of 125 proteins were identified, and the expression profiles of 93 proteins (149 spots) were compared to the mRNA expression profiles. The overall protein expression ratios correlated well with the mRNA ratios between HCC and non-HCC (Pearson's correlation coefficient: $r = 0.73$). Particularly, the HCC/non-HCC expression ratios of proteins involved in metabolic processes showed significant correlation to those of mRNA ($r = 0.9$). A considerable number of proteins were expressed as multiple spots. Among them, several proteins showed spot-to-spot differences in expression level and their expression ratios between HCC and non-HCC poorly correlated to mRNA ratios. Such multi-spotted proteins might arise as a consequence of post-translational modifications.

Keywords: Hepatocellular carcinoma; Proteome; Two-dimensional difference gel electrophoresis; Transcriptome; cDNA microarray

Hepatocellular carcinoma (HCC) is one of the most common cancers worldwide, and a leading cause of death in Africa and Asia [1]. Although several major risks related to HCC, such as hepatitis B and/or hepatitis C virus infection, aflatoxin B1 exposure, and alcohol consumption, and genetic defects, have been revealed [2], the molecular mechanisms leading to the initiation and progression of HCC are not well known. To find the molecular basis of hepatocarcinogenesis, comprehensive gene expression analyses have been done using many systems such as hepatoma cell lines and tissue samples [3,4]. Previously, we have carried out a comprehensive mRNA expression analysis using the serial analysis of gene expression (SAGE) [5] and cDNA microarray-based comparative genomic hybridization [6] to acquire the outline of gene expression profile of HCC. Although these genomic approaches have yielded global gene expression profiles in HCC and identified a number of candidate genes as biomarkers useful for cancer staging, prediction of prognosis, and treatment selection [7], the molecular events accompanying HCC development are not yet understood. In general, proteins rather than transcripts are the major effectors of cellular and tissue function [8] and it is accepted that protein expression do not always correlate with mRNA expression [9,10]. Thus, protein expression analysis, which could complement the available mRNA data, is also important to understand the molecular mechanisms of HCC.

* Corresponding authors. Fax: +81 76 234 4250 (M. Honda), +81 29 856 6136 (Y.Tabuse).
E-mail addresses: mhonda@medf.m.kanazawa-u.ac.jp (M. Honda), y-tabuse@cd.jp.nec.com (Y. Tabuse).

0006-291X/$ - see front matter © 2007 Elsevier Inc. All rights reserved.
doi:10.1016/j.bbrc.2007.11.101

The technique of two-dimensional difference gel electrophoresis (2D-DIGE), developed by Unlu et al. [11] is one of major advances in quantitative proteomics. Several groups have recently utilized 2D-DIGE to examine protein expression changes in HCC samples [12,13], whereas reports on the analysis combining both transcriptomic and proteomic approach are rare.

In the present study, we compared quantitatively protein expression profiles of HCC to non-HCC (non-cancerous liver) samples derived from 14 patients by 2D-DIGE. We also compared the protein expression profiles of the same HCC and non-HCC samples to the mRNA profiles which have been obtained using a cDNA microarray. The expression ratios of 93 proteins showed significant correlations with the mRNA ratios between HCC and non-HCC. Proteins involved in metabolic processes showed more prominent correlation. Our study describes an outline of gene and protein expression profiles in HCC, thus providing us a basis for better understanding of the disease.

Materials and methods

Patients. A total of 14 HCC patients who had surgical resection done in the Kanazawa University Hospital were enrolled. The clinicopathological characteristics of them are shown in Table 1. The HCC samples and adjacent non-tumor liver samples were snap frozen in liquid nitrogen, and used for cDNA microarray and 2D-DIGE analysis. All HCC and non-tumor samples were histologically diagnosed and quantitative detection of hepatitis C virus RNA by Amplicore analysis (Roche Diagnostic Systems) showed positive. The grading and staging of chronic hepatitis associated with non-tumor lesion were histologically assessed according to the method described by Desmet et al. [14] and histological typing of HCC was assessed according to Ishak et al. [15]. All strategies used for gene expression and protein expression analysis were approved by the Ethical Committee of Kanazawa University Hospital.

Preparation of cDNA microarray slides. In addition to in-house cDNA microarray slides consisting of 1080 cDNA clones as previously described [6,16–18], we made new cDNA microarray slides for detailed analysis of the signaling pathway of metabolism and enzyme function in liver disease [19]. Besides cDNA microarray analysis, a total of 256,550 tags were obtained from hepatic SAGE libraries (derived from normal liver, CH-C, CH-C related HCC, CH-B, and CH-B related HCC), including 52,149 unique tags. Among these, 16,916 tags expressing more than two hits were selected to avoid the effect of sequencing errors in the libraries. From these candidate genes, 9614 non-redundant clones were obtained from Incyte Genomics (Incyte Corporation), Clontech (Nippon Becton Dickinson), and Invitrogen (Invitrogen). Each clone was sequence validated and PCR amplified by Dragon Genomics (Takara Bio), and the cDNA microarray slides (Liver chip 10k) were constructed using SPBIO 2000 (Hitachi Software) as described previously [6,16–18].

Table 1
Characteristics of patients involved in this study

Patient No.	Age	Sex[a]	Histology of non-tumor lesion[b]	Tumor histology	Viral status
1	64	M	F4A1	Moderate	HCV
2	65	M	F4A1	Well	HCV
3	48	M	F3A1	Moderate	HCV
4	69	F	F4A2	Moderate	HCV
5	66	F	F4A2	Well	HCV
6	45	M	F4A1	Well	HCV
7	75	F	F4A1	Well	HCV
8	46	M	F4A2	Moderate	HCV
9	66	M	F2A2	Well	HCV
10	75	M	F3A1	Moderate	HCV
11	67	F	F4A2	Well	HCV
12	64	M	F4A1	Moderate	HCV
13	68	M	F4A0	Well	HCV
14	74	M	F1A0	Moderate	HCV

[a] M, male; F, female.
[b] F, fibrosis; A, activity.

RNA isolation and antisense RNA amplification. Total RNA was isolated from liver biopsy samples using an RNA extraction kit (Stratagene). Aliquots of total RNA (5 μg) were subjected to amplification with antisense RNA (aRNA) using a Message AmpTM aRNA kit (Ambion) as recommended by the manufacturer. About 25 μg of aRNA was amplified from 5 μg total RNA, assuming that 500-fold amplification of mRNA was obtained. The quality and degradation of the isolated RNA were estimated after electrophoresis using an Agilent 2001 bioanalyzer. In addition, 10 μg of aRNA was used for further labeling procedures.

Hybridization on cDNA microarray slides and image analysis. As a reference for each microarray analysis, aRNA samples prepared from the normal liver tissue from one of the patients were used. Test RNA samples fluorescently labeled with cyanine (Cy) 5 and reference RNA labeled with Cy3 were used for microarray hybridization as described previously [6,16–18]. Quantitative assessment of the signals on the slides was done by scanning on a ScanArray 5000 (General Scanning) followed by image analysis using GenePix Pro 4.1 (Axon Instruments) as described previously [6,16–18].

Protein expression analysis using 2D-DIGE. Protein samples were homogenized with lysis buffer (7 M urea, 2 M thiourea, 4% w/v CHAPS, 0.8 μM aprotinin, 15 μM pepstatin, 0.1 mM PMSF, 0.5 mM EDTA, 30 mM Tris–HCl, pH 8.5) and centrifuged at 13,000 rpm for 20 min at 4 °C. The supernatants were used as protein samples. The protein concentrations were determined with a protein assay reagent (Bio-Rad). The non-HCC and HCC samples (50 μg each) labeled with either Cy3 or Cy5 according to the manufacture's manual were combined and separated on 2-DE gels together with the Cy2-labeled internal standard (IS), which was prepared by mixing equal amounts of all samples. Analytical 2-DE was performed as described previously [20] using Immobiline DryStrip (pH 3–10, 24 cm, GE Healthcare) in the first dimension and 12.5% SDS–polyacrylamide gels (24 × 20 cm) in the second dimension. Samples were run in triplicate to obtain statistically reasonable results. After scanning with a Typhoon 9410 scanner (GE Healthcare), gels were silver stained for protein identification. For protein identification, 400 μg of the IS sample was also separately run on a 2-DE gel and stained with SYPRO Ruby (Invitrogen). All analytical and preparative gel images were processed using ImageQuant (GE Healthcare) and the protein level analysis was done with the DeCyder software (GE Healthcare). To detect phosphoproteins, 400 μg of HCC and non-HCC samples were separately run on 2-DE gels and stained with ProQ Diamond (Invitrogen). After acquiring images, gels were counterstained with SYPRO Ruby to visualize total proteins as described above.

Protein identification. The excised protein spots were in-gel digested with porcine trypsin (Promega). For LC-ESI-IT MS/MS analysis using LCQ Deca XP (Thermo Electron), the digested and dried peptides were dissolved in 10 μl of 0.1% formic acid in 2% acetonitrile (ACN). The dissolved samples were loaded onto C18 silica gel capillary columns (Magic C18, 50 × 0.2 mm), and the elution from the column was directly connected through a sprayer to an ESI-IT MS. Mobile phase A was 2% ACN containing 0.1% formic acid, and mobile phase B was 90% ACN containing 0.1% formic acid. A linear gradient from 5% to 65% of concentration B was applied to elute peptides. The ESI-IT MS was operated in positive ion mode over the range of 350–2000 (m/z) and the database search was carried out against the IPI Human using MASCOT (Matrixscience). The following search parameters were used: the cutting enzyme, trypsin; one missed cleavage allowed, mass tolerance window, ±1 Da, the MS/MS tolerance window, ±0.8 Da; carbamidomethyl cystein and oxidized methionine as fixed and variable modifications, respectively.

Detection of phosphorylated peptide. Possible phosphorylation sites were investigated by MALDI-TOF-MS using monoammonium phosphate (MAP) added matrix mainly according to Nabetani et al. [21]. An additive of MAP was mixed with α-CHCA matrix solution (5 mg/mL, 0.1% TFA, 50% ACN aqueous) to 40 mM in final concentration. Tryptsin digests of the spots positively stained with ProQ were dissolved into 4 μL of 0.1% TFA, 50% ACN aqueous solution and 1 μL of the peptides solution was spotted on the MALDI target plate. After drying up, 1 μL of the MAP matrix was dropped on the dried peptide mixture. Voyager DE-STR (ABI) was used to obtain mass spectra both in negative and positive ion mode. MS peaks that had relatively stronger intensities in negative ion mode than in positive ion mode were selected as candidates for acidically modified peptides.

Results and discussion

We identified 195 spots representing 125 proteins (Suppl. Table 1) and obtained the corresponding mRNA expression data for a total of 93 proteins (149 spots) (Suppl. Table 2). These 93 proteins were classified according to their biological processes and subcellular localizations into categories described by the Gene Ontology Consortium (http://www.geneontology.org/index.shtml) and about a half of them were related to metabolic processes (Fig. 1A). It is a general agreement that proteins with extremely high or low p*I* as well as hydrophobic proteins are difficult to be detected by 2-DE. Being consistent with this notion, our analysis detected many cytoplasmic proteins (Fig. 1B). Therefore, the protein expression data presented here were biased in favor of cytoplasmic and soluble proteins. The protein expression abundance between non-HCC and HCC was calculated using the normalized spot volume, which was the ratio of spot volume relative to IS (Cy3:Cy2 or Cy5:Cy2) and we used the Student's paired *t*-test ($p < 0.05$) to select the protein spots which were expressed differentially between non-HCC and HCC, using 2-DE gel images run in triplicate. The spot volume of a multi-spotted protein was indicated as a total volume by integrating the intensities of multiple spots as was done by Gygi et al. [10]. Comparison of protein expression profiles revealed that several proteins were expressed differentially between HCC and non-HCC. Proteins whose abundances increased >2-fold or decreased <1/2 in HCC are listed in Table 2. While glutamine synthetase, vimentin, annexin A2 and aldo-keto reductase were up-regulated, carbonic anhydrase 2, argininosuccinate synthetase 1, carbonic anhydrase 1, fructose-1,6-bisphosphatase 1, and betaine-homocysteine methyltransferase were down-regulated in HCC. Up- or down-regulation of most of these proteins in HCC has been reported previously [22–27]. Up-regulation of vimentin and annexin A2, and reduced expression of carbonic anhydrase 1 and 2 was suspected to be associated with cellular motility and metastasis [23,24,26].

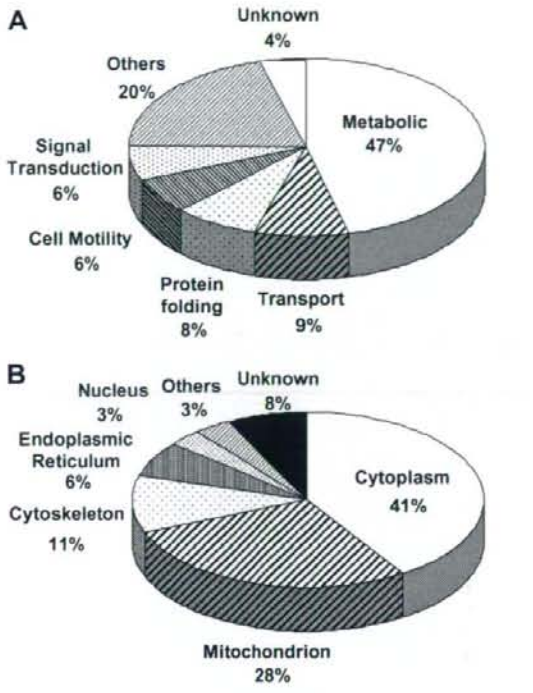

Fig. 1. Classification of identified proteins according to their cellular function (A) and subcellular localization (B).

The mRNA expression abundance was calculated from cDNA microarray data. Hierarchical clustering of

Table 2
Proteins expressed differentially between HCC and non-HCC

Spot ID	Protein name	Refseq ID	Theoretical		Fold change (HCC/non-HCC)		References
			p*I*	MW (kDa)	Protein[a]	mRNA	
1353, 1354	Glutamine synthase	NP_002056.2	6.43	42.7	2.06	3.08	[22]
1039, 1046	Vimentin	NP_003371	5.09	53.6	2.30	1.51	[23]
1716	Annexin A2	NP_001002857.1	7.57	38.8	2.57	1.82	[24]
1685, 1699	Aldo-keto reductase 1B10	NP_064695	7.12	36.2	4.29	4.73	[25]
1977	Carbonic anhydrase 2	NP_000058	6.87	29.3	0.39	0.62	[26]
1307, 1312, 1331	Argininosuccinate synthetase 1	NP_000041.2	8.08	46.8	0.41	0.30	[27]
1941	Carbonic anhydrase 1	NP_001729	6.59	28.9	0.47	1.25	[26]
1582	Fructose-1,6-bisphosphatase 1	NP_000498	6.54	37.2	0.48	0.36	
1256	Betaine-homocysteine methyltransferase	NP_001704	6.41	45.4	0.48	0.40	

[a] Integrated spot volume was used to calculate the fold change of multi-spotted proteins.

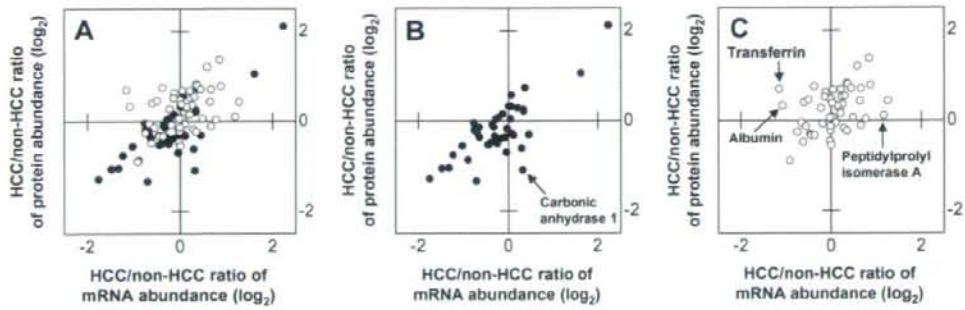

Fig. 2. Comparative analysis of protein and mRNA expression profiles between HCC and non-HCC. (A) The HCC/non-HCC ratios of averaged protein expression levels for 93 proteins were plotted against those of mRNA. Proteins related to metabolic pathways were indicated in closed circles and were shown again in (B). Proteins related to the other biochemical pathways were indicated in open circles and shown in (C). Proteins listed in Table 3 were indicated in (B) and (C). All graphs were depicted in $\log_2$ scale.

Table 3
Proteins whose expression changes between HCC and non-HCC show poor correlation to mRNA expression changes

Spot ID	Protein name	Refseq ID	Theoretical		Spot[a] Av. Ratio	Spot *p* value	Protein ratio	Micro array Av. ratio	Micro array *p* value
			*p*I	MW (kDa)					
564	Transferrin	NP_001054	6.8	79.3	2.23	0.035	1.61	0.45	3.3E−06
565					1.87	0.079			
566					2.28	0.13			
605					0.73	0.098			
1489	Albumin	NP_000468	5.9	71.3	—	0.63	1.25	0.47	2.3E−03
1941	Carbonic anhydrase 1	NP_001729	6.6	28.9	—	3.5E−03	0.47	1.25	0.39
2290	Peptidylprolyl isomerase A	NP_066953	7.7	18.1	—	5.0E−01	1.07	2.29	1.1E−01

[a] Since transferrin was detected in multiple spots, averaged ratio and spot *p* value of each spot is shown.

Table 4
Multi-spotted proteins showing spot-to-spot differences in expression level between non-HCC and HCC

Spot ID	Spot Av. ratio	Spot *p* value	Protein name	Refseq ID	Theoretical		Protein[a] ratio
					*p*I	MW (kDa)	
436	1.92	5.3E−04	Tumor rejection antigen (gp96)	NP_003290	4.8	92.7	1.2
537	0.79	0.16					
564	2.23	0.035	Transferrin	NP_001054	6.8	79.3	1.61
565	1.87	0.079					
566	2.28	0.13					
605	0.73	0.098					
1257	1.02	0.92	Fumarate hydratase	NP_000134	8.8	54.8	0.8
1261	0.6	1.3E−03					

[a] HCC/non-HCC protein ratios were calculated using integrated spot abundances.

gene expression was done with BRB-ArrayTools (http://linus.nci.nih.gov/BRB-ArrayTools.htm). The filtered data were log-transferred, normalized, centered, and applied to the average linkage clustering with centered correlation. BRB-ArrayTools contains a class comparison tool based on univariate *F* tests to find genes differentially expressed between predefined clinical groups. The permutation distribution of the *F* statistic, based on 2000 random permutations, was also used to confirm statistical significance. A *p* value of less than 0.05 for differences in HCC/non-HCC gene expression ratio was considered significant.

The average HCC/non-HCC expression ratios of the 93 proteins were plotted against the mRNA ratios in Fig. 2, where a positive value indicates increased expression in HCC and a negative ratio indicates reduced expression. The overall expression ratio of HCC/non-HCC indicated noticeable correlation between protein and mRNA

(Fig. 2A), and the Pearson's correlation coefficient for this data set (93 proteins/genes) was 0.73. Next, we divided 93 proteins into those related to metabolism and others biological processes. The HCC/non-HCC ratios of protein expression for metabolism-related proteins showed substantial correlation with those of mRNA (Fig. 2B, $r = 0.9$), whereas those of other proteins were poorly correlated (Fig. 2C, $r = 0.36$). Extreme care must be taken in a direct comparison of proteomic data with transcriptome because of multiple layers of discrepancies caused by the distinct sensitivities of cDNA array hybridization and 2-DE, the inability of a cDNA array to distinguish mRNA isoforms and post-translational modifications of proteins. Nevertheless, our results suggest that the expression of considerable portion of proteins with metabolic function listed here is regulated at transcriptional level. On the other hand, post-transcriptional and/or post-translational processes seem to be involved in the regulation of expression level for proteins with other cellular functions as a whole. Four proteins (albumin, transferrin, peptidylproryl isomerase A, and carbonic anhydrase 1) showed apparent poor correlation in protein and mRNA expression profiles (Table 3 and Fig. 2). Transcriptional control might have little effect on the expression changes of these proteins between HCC and non-HCC.

A number of proteins were expressed as multiple spots on 2-DE gels and most multi-spotted proteins showed little spot-to-spot variations in the averaged HCC/non-HCC ratio. Although we do not know how these multiple spots were generated, many of them might be due to the conformational equilibrium of proteins under electrophoresis rather than to any post-translational modifications [28]. On the other hand, the HCC/non-HCC expression ratios of several multi-spotted proteins varied from spot to spot, and three proteins (transferrin, fumarate hydratase, and tumor rejection antigen gp96) were categorized as these multi-spotted proteins (Table 4).

For example, gp96 was detected in two spots (spot #436 and 537) with distinct molecular mass and p*I* and they showed different HCC/non-HCC expression ratio (Fig. 3A and B and Table 4). The expression of these two isoforms was observed to change in the opposite direction between non-HCC and HCC: #436 was up-regulated in HCC (HCC/non-HCC ratio: 1.96) while #537 was down-regulated (HCC/non-HCC ratio: 0.79) (Table 4 and Fig. 3C and D). Gp96 is a glycoprotein present in endoplasmic reticulum and is supposed to function as a molec-

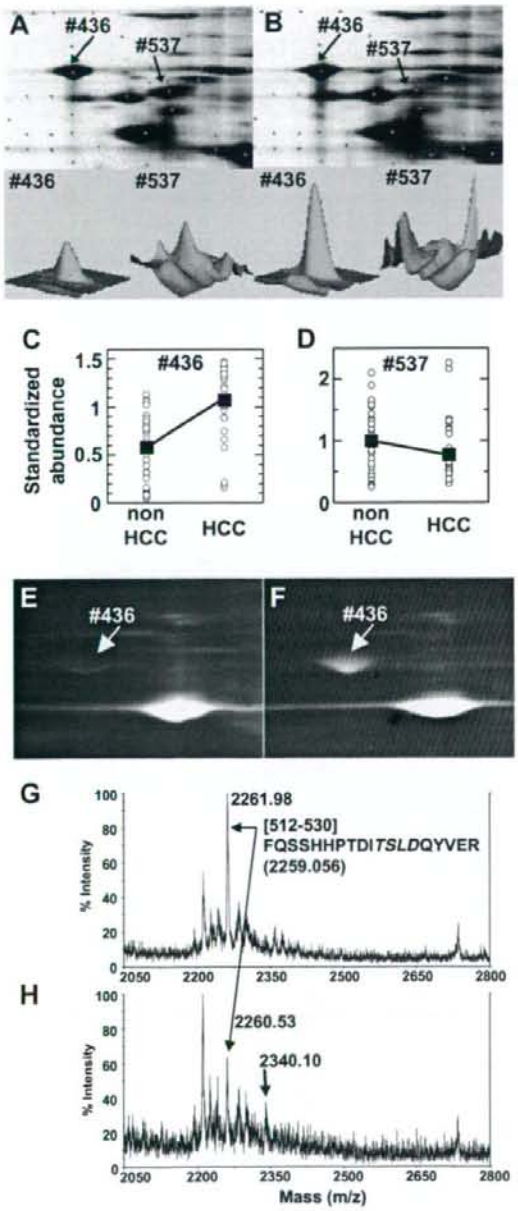

Fig. 3. Comparison of expression profiles of two gp96 spots between HCC and non-HCC. The expression profile and phosphorylation of tumor rejection antigen gp96 in HCC and non-HCC was investigated. Magnified gel images and 3D views of two gp96 spots in non-HCC (A) and HCC (B) were shown. Differences in expression level of two gp96 spots, #436 (C) and #537 (D), between non-HCC and HCC were shown. The open circle indicates the standardized abundance of the individual spot in each sample. The closed square represents the averaged abundance of each gp96 spot. Magnified gel images of non-HCC (E) and HCC (F) stained with ProQ. The #436 spot was positively stained with ProQ, while unambiguous staining of the #537 spot was not observed. Tryptic peptides prepared from the spot #436 were analyzed by MALDI–TOF mass-spectrometry in the positive ion mode (G) and the negative ion mode (H). A peak of 2261.98 detected in positive ion mode corresponds to the amino acid sequence from 512 to 530. In addition to the original peak (*m/z*: 2260.53), a peak mass shifted by +80 Da was detected in the negative ion mode. A predicted phosphorylation consensus motif for protein kinase CK2 is indicated in italics (G).

ular chaperone and intracellular Ca^{2+} regulator [29,30]. Several previous reports have shown that gp96 is glycosylated and phosphorylated, and exists as heterogeneous molecular entities with various molecular weights [31]. In order to know whether gp96 spots were phosphorylated or not, we stained the 2-DE gels with ProQ Diamond which is a dye specific to proteins phosphorylated on serine, threonine or tyrosine residues [32], and has been used successfully to visualize phosphoproteins [33]. We found that the spot #436 was positively stained with ProQ (Fig. 3E and F). We further tried to detect possible phosphorylated peptides in the tryptic digests prepared from #436 by MALDI–TOF–MS according to Nabetani et al. [21]. Searching for those peaks that had relatively stronger intensities in negative ion mode than in positive ion mode, we found two peaks as candidates for acidically modified peptides. They were assigned to the peptides SILFVPTSAPR (amino acid sequence: 385–395, data not shown) and FQSSHHPTDITSLDQYVER (aa512–530). Fig. 3G and H show the unmodified peak and the acidically modified peak (mass shifted by +80 Da in negative ion mode) of the latter peptide, respectively. This peptide contained a predicted phosphorylation consensus motif, [Ser or Thr]-X-X-[Asp or Glu], for protein kinase CK2 (Fig. 3G) which was suggested to phosphorylate gp96 [34]. These results together with ProQ staining indicated that at least one gp96 isoform was phosphorylated and was up-regulated in HCC. Over-expression of gp96 in HCC has been reported previously [35], though the reports that showed over-expression of its phosphorylated form are rare. Further investigation into biological meaning of gp96 phosphorylation may provide us important information about HCC development.

Acknowledgments

We thank the late Dr. A. Tsugita for helpful discussion through this work and N. Tetsura for technical assistance.

Appendix A. Supplementary data

Supplementary data associated with this article can be found, in the online version, at doi:10.1016/j.bbrc.2007.11.101.

References

[1] T.K. Seow, R.C.M.Y. Liang, C.K. Leow, M.C.M. Chung, Hepatocellular carcinoma: from bedside to proteomics, Proteomics 1 (2001) 1249–1263.
[2] L.J. Lopez, J.A. Marrero, Hepatocellular carcinoma, Curr. Opin. Gastroenterol. 3 (2004) 248–253.
[3] H.F. Kawai, S. Kaneko, M. Honda, Y. Shirota, K. Kobayashi, Alpha-fetoprotein-producing hepatoma cell lines share common expression profiles of genes in various categories demonstrated by cDNA microarray analysis, Hepatology 3 (2001) 676–691.
[4] N. Iizuka, M. Oka, H. Yamada-Okabe, N. Mori, T. Tamesa, T. Okada, N. Takemoto, K. Hashimoto, et al., Differential gene expression in distinct virologic types of hepatocellular carcinoma: association with liver cirrhosis, Oncogene 22 (2003) 3007–3014.
[5] T. Yamashita, S. Kaneko, S. Hashimoto, T. Sato, S. Nagai, N. Toyoda, T. Suzuki, K. Kobayashi, et al., Serial analysis of gene expression in chronic hepatitis C and hepatocellular carcinoma, Biochem. Biophys. Res. Commun. 282 (2001) 647–654.
[6] K. Kawaguchi, M. Honda, T. Yamashita, Y. Shirota, S. Kaneko, Differential gene alteration among hepatoma cell lines demonstrated by cDNA microarray-based comparative genomic hybridization, Biochem. Biophys. Res. Commun. 329 (2005) 370–380.
[7] Y. Midorikawa, M. Makuuchi, W. Tang, H. Aburatani, Microarray-based analysis for hepatocellular carcinoma: from gene expression profiling to new challenges, World J. Gastroenterol. 13 (2007) 1487–1492.
[8] N.A. Shackel, D. Seth, P.S. Haber, M.D. Gorrell, G.W. McCaughan, The hepatic transcriptome in human liver disease, Comp. Hepatol. 5 (6) (2006).
[9] T.J. Griffin, S.P. Gygi, T. Ideker, B. Rist, J. Eng, L. Hood, R. Aebersold, Complementary profiling of gene expression at the transcriptome and proteome levels in *Saccharomyces cerevisiae*, Mol. Cell. Proteomics 4 (2002) 323–333.
[10] S.P. Gygi, Y. Rochon, B.R. Franza, R. Aebersold, Correlation between protein and mRNA abundance in yeast, Mol. Cell. Biol. 19 (1999) 1720–1730.
[11] M. Unlu, M.E. Morgan, J.S. Minden, Difference gel electrophoresis: a single gel method for detecting changes in protein extracts, Electrophoresis 11 (1997) 2071–2077.
[12] I.N. Lee, C.H. Chen, J.C. Sheu, H.S. Lee, G.T. Huang, C.Y. Yu, F.J. Lu, L.P. Chow, Identification of human hepatocellular carcinoma-related biomarkers by two-dimensional difference gel electrophoresis and mass spectrometry, J. Proteome Res. 6 (2005) 2062–2069.
[13] C.R. Liang, C.K. Leow, J.C. Neo, G.S. Tan, S.L. Lo, J.W. Lim, T.K. Seow, P.B. Lai, et al., Proteome analysis of human hepatocellular carcinoma tissues by two-dimensional difference gel electrophoresis and mass spectrometry, Proteomics 5 (2005) 2258–2271.
[14] V.J. Desmet, M. Gerber, J.H. Hoofnagle, M. Manns, P.J. Scheuer, Classification of chronic hepatitis: diagnosis, grading and staging, Hepatology 19 (1994) 1513–1520.
[15] K.G. Ishak, P.P. Anthony, L.H. Sobin, Histological typing of tumours of the liver, 2nd ed.WHO International Histological Classification of Tumors, Springer-Verlag, New York, 1994.
[16] M. Honda, S. Kaneko, H. Kawai, Y. Shirota, K. Kobayashi, Differential gene expression between chronic hepatitis B and C hepatic lesion, Gastroenterology 120 (2001) 955–966.
[17] H.F. Kawai, S. Kaneko, M. Honda, Y. Shirota, K. Kobayashi, Alpha-fetoprotein-producing hepatoma cell lines share common expression profiles of genes in various categories demonstrated by cDNA microarray analysis, Hepatology 33 (2001) 676–691.
[18] M. Honda, H. Kawai, Y. Shirota, T. Yamashita, T. Takamura, S. Kaneko, cDNA microarray analysis of autoimmune hepatitis, primary biliary cirrhosis and consecutive disease manifestation, J. Autoimmun. 25 (2005) 133–140.
[19] M. Honda, T. Yamashita, T. Ueda, H. Takatori, R. Nishino, S. Kaneko, Different signaling pathways in the livers of patients with chronic hepatitis B or chronic hepatitis C, Hepatology 44 (2006) 1122–1138.
[20] Y. Tabuse, T. Nabetani, A. Tsugita, Proteomic analysis of protein expression profiles during *Caenorhabditis elegans* development using 2D-difference gel electrophores, Proteomics 5 (2005) 2876–2891.
[21] T. Nabetani, K. Miyazaki, Y. Tabuse, A. Tsugita, Analysis of acidic peptides with a matrix-assisted laser desorption/ionization mass spectrometry using positive and negative ion modes with additive monoammonium phosphate, Proteomics 6 (2006) 4456–4465.
[22] Y. Kuramitsu, T. Harada, M. Takashima, Y. Yokoyama, I. Hidaka, N. Iizuka, T. Toda, M. Fujimoto, et al., Increased expression and phosphorylation of liver glutamine synthetase in well-differentiated

hepatocellular carcinoma tissues from patients infected with hepatitis C virus, Electrophoresis 27 (2006) 1651–1658.
[23] L. Hu, S.H. Lau, C.H. Tzang, J.M. Wen, W. Wang, D. Xie, M. Huang, Y. Wang, et al., Association of Vimentin overexpression and hepatocellular carcinoma metastasis, Oncogene 23 (2004) 298–302.
[24] Z. Dai, Y.K. Liu, J.F. Cui, H.L. Shen, J. Chen, R.X. Sun, Y. Zhang, X.W. Zhou, Identification and analysis of altered alpha1,6-fucosylated glycoproteins associated with hepatocellular carcinoma metastasis, Proteomics 6 (2006) 5857–5867.
[25] E. Zeindl-Eberhart, S. Haraida, S. Liebmann, P.R. Jungblut, S. Lamer, D. Mayer, G. Jäger, S. Chung, H.M. Rabes, Detection and identification of tumor-associated protein variants in human hepatocellular carcinomas, Hepatology 39 (2004) 540–549.
[26] W.H. Kuo, W.L. Chiang, S.F. Yang, K.T. Yeh, C.M. Yeh, Y.S. Hsieh, S.C. Chu, The differential expression of cytosolic carbonic anhydrase in human hepatocellular carcinoma, Life Sci. 73 (2003) 2211–2223.
[27] P.N. Cheng, T.L. Lam, W.M. Lam, S.M. Tsui, A.W. Cheng, W.H. Lo, Y.C. Leung, Pegylated recombinant human arginase (rhArg-peg5,000mw) inhibits the in vitro and in vivo proliferation of human hepatocellular carcinoma through arginine depletion, Cancer Res. 67 (2007) 309–317.
[28] F.S. Berven, O.A. Karisen, J.C. Murrell, H.B. Jensen, Multiple polypeptide forms observed in two-dimensional gels of Methylococcus capsulatus (Bath) polypeptides are generated during the separation procedure, Electrophoresis 24 (2003) 757–761.
[29] J. Melnick, S. Aviel, Y. Argon, The endoplasmic reticulum stress protein GRP94, in addition to BiP, associates with unassembled immunoglobulin chains, J. Biol. Chem. 267 (1992) 21303–21306.
[30] H. Liu, E. Miller, B. van de Water, J.L. Stevens, Endoplasmic reticulum stress proteins block oxidant-induced Ca^{2+} increases and cell death, J. Biol. Chem. 273 (1998) 12858–12862.
[31] A.M. Feldweg, P.K. Srivastava, Molecular heterogeneity of tumor rejection antigen/heat shock protein GP96, Int. J. Cancer 63 (1995) 310–314.
[32] T.H. Steinberg, B.J. Agnew, K.R. Gee, W.-Y. Leung, T. Goodman, B. Schulenberg, J. Hendrickson, J.M. Beechem, R.P. Haugland, W.F. Patton, Global quantitative phosphoprotein analysis using multiplexed proteomics technology, Proteomics 3 (2003) 1128–1144.
[33] B.R. Chitteti, Z. Peng, Proteome and phosphoproteome dynamic change during cell dedifferentiation in Arabidopsis, Proteomics 7 (2007) 1473–1500.
[34] S.E. Cala, GRP94 hyperglycosylation and phosphorylation in Sf21 cells, Biochim. Biophys. Acta 1496 (2000) 296–310.
[35] D.F. Yao, X.H. Wu, X.Q. Su, M. Yao, W. Wu, L.W. Qiu, L. Zou, X.Y. Meng, Abnormal expression of HSP gp96 associated with HBV replication in human hepatocellular carcinoma, Hepatobiliary Pancreat. Dis. Int. 5 (2006) 381–386.

ELSEVIER

Journal of Hepatology 48 (2008) 736–742

Journal of Hepatology

www.elsevier.com/locate/jhep

The presence of steatosis and elevation of alanine aminotransferase levels are associated with fibrosis progression in chronic hepatitis C with non-response to interferon therapy☆

Masayuki Kurosaki[1], Kotaro Matsunaga[1], Itsuko Hirayama[1], Tomohiro Tanaka[1], Mitsuaki Sato[1], Nobutoshi Komatsu[1], Naoki Umeda[1], Takanori Hosokawa[1], Ken Ueda[1], Kaoru Tsuchiya[1], Hiroyuki Nakanishi[1], Jun Itakura[1], Yasuhiro Asahina[1], Shozo Miyake[1], Nobuyuki Enomoto[2], Namiki Izumi[1,*]

[1]*Division of Gastroenterology and Hepatology, Musashino Red Cross Hospital, 1-26-1 Kyonan-cho, Musashino-shi, Tokyo 180-8610, Japan*
[2]*First Department of Internal Medicine, University of Yamanashi, Yamanashi, Japan*

***Background/Aims*: Interferon (IFN) therapy leads to regression of hepatic fibrosis in chronic hepatitis C patients who achieve a sustained virologic response (SVR), while the beneficial effect is limited in those who fail to do so. The aim of the present study was to define factors associated with progression of fibrosis in patients who do not achieve a SVR.**

***Methods*: Fibrosis staging scores were compared between paired liver biopsies before and after IFN in 97 chronic hepatitis C patients who failed therapy. The mean interval between biopsies was 5.9 years. Factors associated with progression of fibrosis were analyzed.**

***Results*: Fibrosis progressed in 23%, remained unchanged in 47% and regressed in 29%. Steatosis and a high average alanine aminotransferase (ALT) between biopsies were independent factors for progression of fibrosis with risk ratios of 5.53 and 4.48, respectively. Incidence and yearly rate of progression of fibrosis was 64% and 0.22 ± 0.29 fibrosis units per year in those with both risk factors compared to 8% and -0.04 ± 0.17 fibrosis units per year in those negative for both factors.**

***Conclusions*: Hepatic steatosis and elevated ALT levels are risk factors for progression of fibrosis in chronic hepatitis C patients who fail to achieve a SVR to IFN therapy and therefore may be therapeutic targets to halt the potentially progressive disease.**

***Keywords*: Steatosis; ALT; Fibrosis**

1. Introduction

Hepatitis C virus (HCV) is a major cause of chronic liver disease worldwide. Mortality associated with HCV infection results from the development of liver cirrhosis and hepatocellular carcinoma, which now is the leading indication for liver transplantation [1]. Treatment with interferon (IFN), alone or in combination with ribavirin (RBV), can eradicate HCV infection in some patients, leading to sustained nor-

Received 20 July 2007; received in revised form 8 October 2007; accepted 17 December 2007; available online 26 February 2008
Associate Editor: J.G. McHutchison

☆ The authors who have taken part in the research of this paper declared that they do not have a relationship with the manufactures of the drug involved either in the past or present and they did not receive funding from the manufactures to carry out their research. They did not receive funding from any source to carry out this study.

* Corresponding author. Tel.: +81 422 32 3111; fax: +81 422 32 9551.
E-mail address: nizumi@musashino.jrc.or.jp (N. Izumi).

0168-8278/$34.00
doi:10.1016/j.jhep.2007.12.025

malization of liver function, improvement of hepatic inflammation and fibrosis and a decreased risk of the development of hepatocellular carcinoma [2,3]. The problem is that only 50% of patients achieve a sustained virological response (SVR) to therapy even with the most highly developed regimens of IFN [4,5]. The remaining patients who fail to clear the virus are left with the risk of progressive disease. In order to halt this potentially progressive disease, there is a need to establish an effective target of therapeutic intervention independent of antiviral therapy. Therefore, it is important to define risk factors for the progression of fibrosis among chronic hepatitis C patients who do not achieve a SVR to IFN therapy.

Several factors that may affect the rate of progression of fibrosis have been investigated extensively, including older age at infection, male gender, obesity, heavy alcohol consumption, and a high grade of necroinflammation [6–8]. Several cross-sectional and longitudinal studies suggest that hepatic steatosis, which is a common histological feature of chronic hepatitis C [9], influences the progression of hepatic fibrosis [10–14], while other studies did not find such an association [15–18]. Besides these conflicting results, no study to date has reported the effect of steatosis on longitudinal progression of fibrosis among patients who fail to respond to IFN therapy. Therefore, we studied factors associated with progression of fibrosis in those who failed IFN therapy by comparing paired pre-treatment and post-treatment liver biopsies.

2. Methods

2.1. Patients

The aim of the study was to identify risk factors associated with progression of fibrosis in chronic hepatitis C patients who failed to achieve a SVR to IFN therapy. To be included in this retrospective study, patients had to have undergone liver biopsy before and after therapy, been treated with IFN and not achieved a SVR. Patients with alcohol consumption of more than 20 g per day, co-infected with HBV or HIV, and those with another known aetiology of liver disease, such as autoimmune hepatitis or metabolic disorders, were excluded. A database of patients who had undergone liver biopsy at Musashino Red Cross Hospital between 1990 and 2004 was reviewed retrospectively and a total of 1241 chronic hepatitis C patients treated with IFN were identified; of these, 407 had a SVR and 834 had not achieved a SVR. Among those with treatment failure, 104 fulfilled the above criteria but seven patients with cirrhosis before treatment were excluded because the endpoint of the study was progression of fibrosis. Therefore, this study cohort consisted of 97 patients. In these patients, second liver biopsies were performed before the second course of IFN therapy. Otherwise, there were no standardized indications for the second liver biopsy which may be the limitation of our study. Demographic characteristics of patients at the time of initial biopsy are shown in Table 1. The time between the paired biopsies was 5.9 years on average, with a range of 1.2–11.6 years. The median interval between first biopsy and IFN therapy was 3 days (range 2–93 days), and that between completion of IFN therapy and second biopsy was 5.4 years (range 0.8–11.2 years). Laboratory tests were performed monthly or bimonthly in all patients and all measurements were taken at our single hospital.

Table 1
Demographic characteristics of patients

Number of patients	97
Age (years)	52 ± 9
Gender: male/female	50/47
BMI (kg/m^2)	23.9 ± 3.2 (median 24.0, range19–33)
BMI <25/25–30/30 ≤ (kg/m^2)	55/37/5
Route of transmission	
Blood transfusion/unknown	38/59
Duration of infection (years)	30.4 ± 9.2 (median 33.5, range 3–48)
Genotype 1b/2a/2b	85/4/8
Serum HCV-RNA (Meq/ml)	7.7 ± 9.7
Pretreatment AST (IU/l)	73 ± 40
Pretreatment ALT (IU/l)	104 ± 69
Pretreatment GGT (IU/l)	51 ± 44
Histological variables at first biopsy	
Stage of fibrosis 1/2/3	33/38/26
Grade of activity 0/1/2/3	15/36/41/5
Grade of steatosis 0/1/2/3	21/37/25/14
Size of steatosis macro/micro/mixed	16/17/64
Localization of steatosis centrilobular/diffuse	3/94

BMI, body mass index; AST, aspartate aminotransferase, normal range is 7–38 IU; ALT, alanine aminotransferase, normal range is 4–43 IU/l; GGT, gamma-glutamyltransferase, normal range is 0–73 IU/l; macro, macro-vesicular steatosis; micro, micro-vesicular steatosis.

2.2. Histological evaluation

Median length of biopsy specimen and number of portal tracts were 13.0 mm (range 10–40 mm) and 12 (range 6–34). All liver biopsy specimens were evaluated separately by three independent pathologists who were blinded to the clinical data. If there was discordance, the scores assigned by two pathologists were used for the analysis. Fibrosis and activity were scored according to the METAVIR scoring system [19]. Fibrosis was staged on a scale of 0–4; F0 (no fibrosis), F1 (mild fibrosis: portal fibrosis without septa), F2 (moderate fibrosis: few septa), F3 (severe fibrosis: numerous septa without cirrhosis) and F4 (cirrhosis). Activity of necroinflammation was graded on a scale of 0–3: A0 (no activity), A1 (mild activity), A2 (moderate activity) and A3 (severe activity). Percentage of steatosis was quantified by determining the average proportion of hepatocytes affected by steatosis and was graded on a scale of 0–3: grade 0 (no steatosis), grade 1 (0–9%), grade 2 (10–29%), and grade 3 (over 30%). Size of steatosis was categorized into micro-vesicular, macro-vesicular and mixed types. Localization of steatosis was categorized into either centrilobular or diffuse pattern. Definition of changes in the grade of steatosis was as follows: worsening as 1 point or more increase, improvement as 1 point or more decrease, and stability as no change.

2.3. Changes in fibrosis-staging score overtime

Changes in progression of fibrosis were defined as follows: progression of fibrosis was defined as a 1 point or more increase, regression as a 1 point or more decrease and stability as no change in the METAVIR fibrosis-staging score. In addition, because the time between paired biopsies was variable, the yearly rate of progression of fibrosis was calculated as the change in fibrosis-staging score divided by the time between paired biopsies, as originally described by Poynard et al. [6].

2.4. Statistical analysis

The STAT View software package was used for statistical analysis. Categorical data were analyzed using the Fisher's exact test. Continuous variables were compared with the Student's t test. Variables that were statistically significant in univariate analysis were included in multivariate analysis using logistic regression analysis. The Kaplan–Meier method and log-rank test were used to analyze the time to occurrence of fibrosis progression. A p-value of less than 0.05 was considered statistically significant.

3. Results

3.1. Factors associated with the initial stage of fibrosis (cross-sectional study)

All three pathologists assigned the same score in 85% of patients for fibrosis staging and 95% of patients for steatosis-grading. In cases with discordance, at least two pathologists assigned the same scale. The stage of fibrosis in the initial liver biopsy was F1 in 33, F2 in 38 and F3 in 26 patients. Various clinical factors were analyzed in association with the advanced stage of fibrosis. As a result, the presence of F3 fibrosis was associated with older age, (51 ± 9 in F1–2 vs. 55 ± 9 in F3, $p = 0.03$), higher grade of histological activity (A2–3 was 35% in F1–2 vs. 84% in F3, $p = 0.0001$) and higher grade of steatosis (steatosis grade 2–3 was 34% in F1–2 vs. 58% in F3, $p = 0.04$).

The grade of steatosis was 0 in 21, 1 in 37, 2 in 25 and 3 in 14 patients. A higher grade of steatosis was associated with female gender (the male/female ratio was 35/23 in grade 0–1 vs. 15/24 in grade 2–3, $p = 0.04$), increased BMI (BMI over 25 kg/m^2 was 31% in grade 0–1 vs. 62% in grade 2–3, $p = 0.006$), and higher grade of histological activity (A2–3 was 38% in grade 0–1 vs. 62% in grade 2–3, $p = 0.03$). Multivariate logistic regression analysis revealed that increased BMI and female gender were independent factors associated with a high grade of steatosis (Table 2).

Table 2
Multivariate logistic regression analysis of factors associated with hepatic steatosis

	Odds	95% C.I.	p Value
BMI			
⩾25 kg/m^2	4.23	1.63–10.95	0.003
Gender			
Female	2.75	1.06–7.14	0.04
Activity grade			
2–3	2.30	0.85–6.26	0.10
Fibrosis stage			
3	1.63	0.53–4.97	0.39

3.2. Change in fibrosis-staging scores over time (longitudinal study)

Fibrosis staging progressed in 23% (progression by 2 points in 5% and 1 point in 18%), remained unchanged in 47% and regressed in 29% (regression by 2 points in 2% and 1 point in 27%). At first liver biopsy, laparoscopy was performed in 73 patients and the presence of cirrhosis (F4) was carefully excluded. In another 24 patients, the possibility of mis-diagnosis of F4 as F3 remains. However, the incidence of fibrosis progression did not differ according to the initial stage of fibrosis (21.2% in F1, 26.3% in F2 and 19.2% in F3, $p = 0.78$) which indicates that misdiagnosis of F4 as F3 at initial biopsy is unlikely.

Among various factors, as shown in Table 3, a higher grade of steatosis, higher levels of ALT and AST (average value for the period between the paired liver biopsies) were associated with progression of fibrosis. Since there was significant correlation between ALT and AST levels ($r = 0.684$, $p < 0.0001$), these two variables could not be analyzed together in multivariate analysis.

Table 3
Factors associated with the progression of fibrosis over time

	Progression $n = 22$	Non-progression $n = 75$	p Value
Gender: male/female	9/13	41/34	0.33
Age at biopsy: <60/⩾60 years	14/8	59/16	0.17
HCV genotype: 1b/non-1b	19/3	66/9	0.99
BMI: <25/⩾25 kg/m^2	11/11	44/31	0.48
Duration of infection (years)	32.1 ± 5.2	29.9 ± 10.0	0.56
Activity on first biopsy			
Grade: 0–1/2–3	8/14	43/32	0.10
Steatosis on first biopsy			
Grade: 0–1/2–3	6/16	52/23	0.001
Size: macro/micro/mixed	4/4/14	12/13/50	0.96
Location: centrilobular/diffuse	1/21	2/73	0.54
Evolution of steatosis			
Worsening/improvement/stable	2/2/18	9/8/58	0.09
Average ALT: <100/⩾100 IU/l	13/9	67/8	0.003
Average AST: <75/⩾75 IU/l	10/12	61/14	0.002
Interval between biopsies (years)	5.1 ± 3.2	6.2 ± 2.4	0.09
Interval between completion of IFN and second biopsy (years)	4.6 ± 3.2	5.7 ± 2.4	0.10
Treatment regimen			
RBV−/RBV+	22/0	71/4	0.27
Response to IFN			
Relapser/non-responder	16/6	53/22	0.99
Evolution of weight			
Gain/loss/stable	5/8/9	29/21/25	0.38

macro, macro-vesicular steatosis; micro, micro-vesicular steatosis; RBV−, interferon monotherapy; RBV+, interferon plus ribavirin combination therapy.
Duration of infection was determined in 38 patients whose source of infection was blood transfusion.

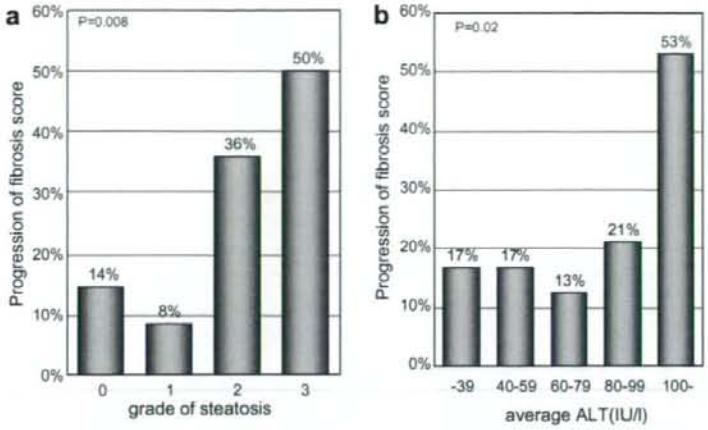

Fig. 1. Progression of fibrosis stage, hepatic steatosis and the average level of ALT. The progression of the fibrosis score over time is illustrated using bar charts. (a) Steatosis grades of 2 or 3 at initial liver biopsy were associated with the increased progression of fibrosis over time. (b) High average ALT levels during the observation period were associated with progression of fibrosis at the threshold of 100 IU/l.

Thus, average level of ALT was used for the following analysis. The probability of progression of fibrosis was 14%, 8%, 36% and 50% in patients with steatosis grades of 0, 1, 2 and 3, respectively ($p = 0.008$), and 17%, 17%, 13%, 21% and 53% in patients with average ALT values of <40, 40–59, 60–79, 80–99 and over 100 IU/l, respectively ($p = 0.02$) (Fig. 1). Multivariate logistic regression analysis revealed that these two were independent risk factors associated with the progression of fibrosis with risk ratios of 5.14 for steatosis ($p = 0.004$) and 5.21 for ALT ($p = 0.01$) (Table 4).

When patients were categorized in terms of these two risk factors, the incidence of progression of fibrosis was as high as 64% in those with both risk factors, compared to 8% in those negative for these factors. Conversely, the incidence of fibrosis regression was only 9% in those with both risk factors, compared to 37% in those negative for these factors ($p = 0.0003$) (Fig. 2).

In order to adjust for the effect of variable intervals between paired biopsies, the yearly rate of progression of fibrosis was calculated as the change in the fibrosis-staging score divided by the time between paired biopsies. The average of all patients was 0.02 ± 0.22 fibrosis units per year. Again, a higher grade of steatosis ($p = 0.004$) and higher average level of ALT ($p = 0.0005$) were associated with a higher rate of progression of fibrosis (Table 5). In addition, the yearly rate of progression of fibrosis was 0.22 ± 0.29 fibrosis units per year in those with both risk factors, 0.12 ± 0.37 in those with elevated ALT alone, 0.05 ± 0.16 in those with steatosis alone and -0.05 ± 0.17 in those negative for these two factors ($p = 0.001$). Time to progression of fibrosis at second biopsy was also analyzed by the Kaplan–Meier method. The cumulative probabilities of progression of fibrosis at five years were 58% in those with both risk factors, 33% in those with elevated ALT alone, 18% in those with steatosis alone and 2% in those negative for these two factors ($p < 0.0001$) (Fig. 3).

Table 4
Multivariate logistic regression analysis of factors associated with progression of fibrosis over time

	Odds	95% C.I.	*p* Value
Steatosis grade ≥2	5.14	1.67–15.77	0.004
Average ALT ≥100 IU/l	5.21	1.49–18.20	0.01

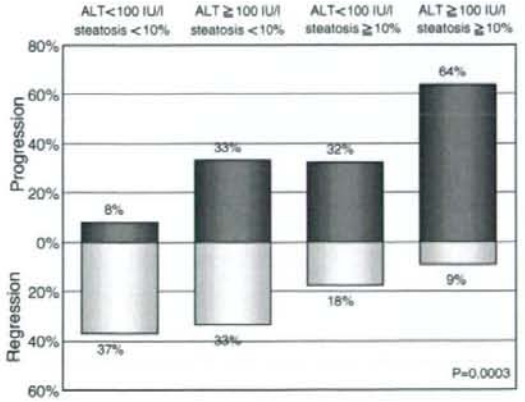

Fig. 2. Evolution of fibrosis stage in terms of risk factors. Patients were categorized into four groups according to the presence or absence of two risk factors. The upper bar chart (dark gray) indicates the progression of fibrosis while the lower bar chart (light gray) indicates the regression of fibrosis.

Table 5
Factors associated with the yearly rate of fibrosis progression

	n	Mean	SD	*p* Value
Gender				
Male	50	−0.01	0.19	0.12
Female	47	0.06	0.23	
Age at biopsy				
<60 years	73	−0.0002	0.21	0.06
≥60 years	24	0.10	0.23	
HCV genotype				
1b	83	0.02	0.20	0.37
non-1b	14	0.08	0.32	
BMI				
<25 kg/m^2	53	0.004	0.24	0.32
≥25 kg/m^2	44	0.05	0.19	
Steatosis on first biopsy				
0–1	58	−0.03	0.20	0.004
2–3	39	0.10	0.21	
Activity on first biopsy				
0–1	51	−0.001	0.21	0.24
2–3	46	0.05	0.22	
Fibrosis on first biopsy				
1–2	71	0.03	0.20	0.43
3	26	−0.01	0.25	
Average ALT between paired biopsies				
<100 IU/l	80	−0.01	0.17	0.0005
≥100 IU/l	17	0.18	0.31	

4. Discussion

In the present study, we found that a higher grade of hepatic steatosis at baseline and a higher average value of ALT are independent risk factors for the progression of fibrosis over time in chronic hepatitis C patients who fail to achieve a SVR to IFN therapy. These two factors may be involved in promoting the progression of fibrosis. The association between steatosis and progression of fibrosis in untreated patients had been suggested by previous studies but this study is the first to demonstrate a similar association for treated patients. These findings are particularly important to establish a rationale for identifying therapeutic targets to halt potentially progressive disease independent of antiviral therapy.

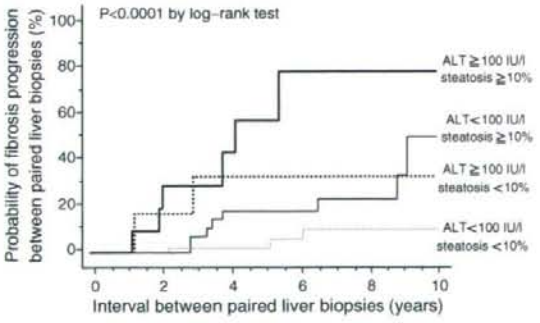

Fig. 3. Probability of fibrosis progression according to the presence of risk factors. Patients were categorized into four groups according to the presence or absence of two risk factors and the time to progression of fibrosis was analyzed.

There have been many studies that analyzed the association between steatosis and progression of liver fibrosis in HCV-infected patients, and the majority have shown a positive association [10–13], including a large scale meta-analysis [14]. However, some studies did not report this association [15–18]. There are two possible reasons for these conflicting results. First, longitudinal studies, rather than cross-sectional studies, are particularly important in the analysis of the role of steatosis in time-dependent progression of hepatic fibrosis, because cross-sectional studies involve patients with an unknown duration of steatosis. Three of four longitudinal studies that analyzed the progression of fibrosis through paired biopsies in untreated patients showed that the presence or worsening of steatosis was associated with the progression of fibrosis [12,13,20], and the probability of progression of fibrosis was significantly related to the grade of steatosis [13]. In one study, however, progression of fibrosis was correlated with older age, periportal necroinflammation and ALT elevations but not with steatosis [17]. Interestingly, steatosis was associated with older age, higher body mass index and ALT elevations in that study, indicating an indirect association of steatosis and fibrosis progression. The authors assumed that steatosis was the result rather than the cause of inflammation. This observation highlights the second reason for the controversies over a correlation between the presence of steatosis and progression of fibrosis, that is, there are so many confounding factors associated with both steatosis and fibrosis progression such as older age, advanced stage of fibrosis, higher degree of inflammation, elevated ALT, increased body mass index and insulin resistance. Because it is very difficult to prove a causal relationship between these confounding factors through clinical observations, steatosis may be a hallmark of the progression of fibrosis but it is unclear whether the effect of steatosis on progression of fibrosis is direct or mediated by other confounding factors.

Hepatic steatosis is a common pathological finding in patients with chronic hepatitis C [9]. Because the proportion of patients with steatosis is higher than would be expected from a chance association, a direct role of HCV in the pathogenesis of steatosis is suggested, at least in some patients with genotype 3 infection [21]. Furthermore, other observations suggest that steatosis may be metabolic; it is correlated with a high body mass index, visceral adiposity and insulin resistance, especially in non-3a genotypes and metabolic steatosis also is correlated with progression of fibrosis [11,22]. The

most reliable evidence that metabolic steatosis is associated with progression of fibrosis is shown by a study indicating that weight reduction in patients with chronic hepatitis C leads to a reduction in steatosis and an improvement in fibrosis, despite the persistence of HCV infection. A reduction in steatosis was significantly associated with a decrease in stellate cell activation and regression of hepatic fibrosis in 56% of patients. Thus, weight reduction may provide an important new adjunct treatment strategy for patients with chronic hepatitis C [23]. A recent study showed that the administration of pioglitazone led to metabolic and histological improvement in subjects with non-alcoholic steatohepatitis [24]. Whether amelioration of insulin resistance could improve steatosis and fibrosis in chronic hepatitis C awaits future investigation.

The mechanism by which steatosis could aggravate hepatic fibrosis in chronic hepatitis C patients remains largely hypothetical. Steatosis related insulin resistance may contribute to hyperinsulinemia and increased hepatic expression of connective tissue growth factor leading to progression of fibrosis [25]. Alternatively, a steatohepatitis-like pathway may be involved where steatosis requires a second hit for progression to fibrosis [26]. The most likely candidate is an oxidative stress with subsequent lipid peroxidation which is reported to correlate with the stage of fibrosis [27]. Another important candidate is an antiviral inflammatory response. It is reported that steatotic liver has increased susceptibility to inflammatory response [28] and that a higher grade of steatosis is correlated with a higher degree of inflammation or elevated ALT [14,15,17]. Higher degree of inflammation or elevated ALTs are associated with the progression of fibrosis [29,30], but hepatic steatosis may be responsible for the amplification of hepatic inflammation and vice versa, and the coexistence of these two factors may lead to further progression of fibrosis, as in patients with non-alcoholic steatohepatitis. In our study, average value of ALT between two biopsies was associated with fibrosis progression, whereas histological inflammation at first liver biopsy was not. The reason for this discordance may be explained by the dynamic process of hepatic necroinflammation. Severity of histological inflammation at the time of biopsy may not reflect subsequent inflammation process, whereas average value of regularly determined ALT may reflect entire fluctuation of hepatic inflammation. If so, our finding may support the hypothesis that co-operation of steatosis as the first hit and dynamic process of hepatic inflammation as the second hit promotes fibrosis progression. On the other hand, elevation of ALT may not be a mere reflection of hepatic inflammation so much as hepatocellular death such as apoptosis. Since it is reported that apoptotic caspase activation is elevated in HCV-associated steatosis [31] and that steatotic liver has increased susceptibility to apoptosis [28], elevation of ALT may also reflect an apoptosis amplified by steatosis which may lead to fibrosis progression.

Regardless of the precise mechanism, the results of the present study suggest that lowering of ALT levels may be beneficial in preventing progression of fibrosis in patients who failed to achieve a SVR. In our population, all patients received 24 weeks of IFN therapy and none received long-term maintenance therapy aiming to ameliorate hepatic inflammation. However, we speculate that amelioration of hepatic inflammation and lowering ALT levels by long-term IFN may prevent fibrosis progression in patients who remain viremic since it has been reported that IFN slowed the natural progression of fibrosis in patients who failed IFN therapy when the rate of progression of fibrosis after IFN therapy was compared to the estimated rate of progression before therapy [2,32], and that treatment duration was associated with the reduction of fibrosis independent of virological response [2]. Another possible approach to lower ALT levels may be the use of ursodeoxycholic acid, which has been reported to induce an almost 30% decrease in serum ALT levels [33,34]. The long-term efficacy of therapies targeted to the reduction of hepatic fibrosis needs future verification.

Some factors related to fibrosis progression in previous studies such as obesity [35] and worsening of steatosis [20] were not significant in our study. In our study where the majority of the population had normal body weight and very few had obesity (BMI $\geqslant 30\ kg/m^2$), impact of increased BMI on fibrosis progression may not be evaluated. Also, a smaller number of patients with worsening of steatosis (11.3% in present study and 34% in previous study [20]) may be the reason for the discrepancy. This may be due to difference in patient selection since no patients in that study had antiviral treatment between two biopsies.

In conclusion, the presence of hepatic steatosis and elevated ALT levels are risk factors for progression of fibrosis in chronic hepatitis C patients who failed to achieve a SVR to IFN therapy. These two factors may be a therapeutic target to halt the potentially progressive disease independent of antiviral therapy.

References

[1] Liang TJ, Rehermann B, Seeff LB, Hoofnagle JH. Pathogenesis, natural history, treatment, and prevention of hepatitis C. Ann Intern Med 2000;132:296–305.

[2] Poynard T, McHutchison J, Davis GL, Esteban-Mur R, Goodman Z, Bedossa P, et al. Impact of interferon alfa-2b and ribavirin on progression of liver fibrosis in patients with chronic hepatitis C. Hepatology 2000;32:1131–1137.

[3] Yoshida H, Shiratori Y, Moriyama M, Arakawa Y, Ide T, Sata M, et al. Interferon therapy reduces the risk for hepatocellular carcinoma: national surveillance program of cirrhotic and noncirrhotic patients with chronic hepatitis C in Japan. IHIT Study Group. Inhibition of Hepatocarcinogenesis by Interferon Therapy. Ann Intern Med 1999;131:174–181.

[4] Manns MP, McHutchison JG, Gordon SC, Rustgi VK, Shiffman M, Reindollar R, et al. Peginterferon alfa-2b plus ribavirin compared with interferon alfa-2b plus ribavirin for initial treatment of chronic hepatitis C: a randomised trial. Lancet 2001;358:958–965.

[5] Fried MW, Shiffman ML, Reddy KR, Smith C, Marinos G, Goncales Jr FL, et al. Peginterferon alfa-2a plus ribavirin for chronic hepatitis C virus infection. N Engl J Med 2002;347:975–982.

[6] Poynard T, Bedossa P, Opolon P. Natural history of liver fibrosis progression in patients with chronic hepatitis C. The OBSVIRC, METAVIR, CLINIVIR, and DOSVIRC groups. Lancet 1997;349:825–832.

[7] Marcellin P, Asselah T, Boyer N. Fibrosis and disease progression in hepatitis C. Hepatology 2002;36:S47–S56.

[8] Alberti A, Vario A, Ferrari A, Pistis R. Review article: chronic hepatitis C – natural history and cofactors. Aliment Pharmacol Ther 2005;22 Suppl 2:74–78.

[9] Lefkowitch JH, Schiff ER, Davis GL, Perrillo RP, Lindsay K, Bodenheimer Jr HC, et al. Pathological diagnosis of chronic hepatitis C: a multicenter comparative study with chronic hepatitis B. The Hepatitis Interventional Therapy Group. Gastroenterology 1993;104:595–603.

[10] Hourigan LF, Macdonald GA, Purdie D, Whitehall VH, Shorthouse C, Clouston A, et al. Fibrosis in chronic hepatitis C correlates significantly with body mass index and steatosis. Hepatology 1999;29:1215–1219.

[11] Adinolfi LE, Gambardella M, Andreana A, Tripodi MF, Utili R, Ruggiero G. Steatosis accelerates the progression of liver damage of chronic hepatitis C patients and correlates with specific HCV genotype and visceral obesity. Hepatology 2001;33:1358–1364.

[12] Westin J, Nordlinder H, Lagging M, Norkrans G, Wejstal R. Steatosis accelerates fibrosis development over time in hepatitis C virus genotype 3 infected patients. J Hepatol 2002;37:837–842.

[13] Fartoux L, Chazouilleres O, Wendum D, Poupon R, Serfaty L. Impact of steatosis on progression of fibrosis in patients with mild hepatitis C. Hepatology 2005;41:82–87.

[14] Leandro G, Mangia A, Hui J, Fabris P, Rubbia-Brandt L, Colloredo G, et al. Relationship between steatosis, inflammation, and fibrosis in chronic hepatitis C: a meta-analysis of individual patient data. Gastroenterology 2006;130:1636–1642.

[15] Asselah T, Boyer N, Guimont MC, Cazals-Hatem D, Tubach F, Nahon K, et al. Liver fibrosis is not associated with steatosis but with necroinflammation in French patients with chronic hepatitis C. Gut 2003;52:1638–1643.

[16] Hui JM, Sud A, Farrell GC, Bandara P, Byth K, Kench JG, et al. Insulin resistance is associated with chronic hepatitis C virus infection and fibrosis progression [corrected]. Gastroenterology 2003;125:1695–1704.

[17] Perumalswami P, Kleiner DE, Lutchman G, Heller T, Borg B, Park Y, et al. Steatosis and progression of fibrosis in untreated patients with chronic hepatitis C infection. Hepatology 2006;43:780–787.

[18] Conjeevaram HS, Kleiner DE, Everhart JE, Hoofnagle JH, Zacks S, Afdhal NH, et al. Race, insulin resistance and hepatic steatosis in chronic hepatitis C. Hepatology 2007;45:80–87.

[19] Bedossa P, Poynard T. An algorithm for the grading of activity in chronic hepatitis C. The METAVIR Cooperative Study Group. Hepatology 1996;24:289–293.

[20] Castera L, Hezode C, Roudot-Thoraval F, Bastie A, Zafrani ES, Pawlotsky JM, et al. Worsening of steatosis is an independent factor of fibrosis progression in untreated patients with chronic hepatitis C and paired liver biopsies. Gut 2003;52:288–292.

[21] Mihm S, Fayyazi A, Hartmann H, Ramadori G. Analysis of histopathological manifestations of chronic hepatitis C virus infection with respect to virus genotype. Hepatology 1997;25:735–739.

[22] Fartoux L, Poujol-Robert A, Guechot J, Wendum D, Poupon R, Serfaty L. Insulin resistance is a cause of steatosis and fibrosis progression in chronic hepatitis C. Gut 2005;54:1003–1008.

[23] Hickman IJ, Clouston AD, Macdonald GA, Purdie DM, Prins JB, Ash S, et al. Effect of weight reduction on liver histology and biochemistry in patients with chronic hepatitis C. Gut 2002;51:89–94.

[24] Belfort R, Harrison SA, Brown K, Darland C, Finch J, Hardies J, et al. A placebo-controlled trial of pioglitazone in subjects with nonalcoholic steatohepatitis. N Engl J Med 2006;355:2297–2307.

[25] Paradis V, Perlemuter G, Bonvoust F, Dargere D, Parfait B, Vidaud M, et al. High glucose and hyperinsulinemia stimulate connective tissue growth factor expression: a potential mechanism involved in progression to fibrosis in nonalcoholic steatohepatitis. Hepatology 2001;34:738–744.

[26] Day CP, James OF. Steatohepatitis: a tale of two "hits"? Gastroenterology 1998;114:842–845.

[27] Paradis V, Mathurin P, Kollinger M, Imbert-Bismut F, Charlotte F, Piton A, et al. In situ detection of lipid peroxidation in chronic hepatitis C: correlation with pathological features. J Clin Pathol 1997;50:401–406.

[28] Walsh MJ, Vanags DM, Clouston AD, Richardson MM, Purdie DM, Jonsson JR, et al. Steatosis and liver cell apoptosis in chronic hepatitis C: a mechanism for increased liver injury. Hepatology 2004;39:1230–1238.

[29] Mathurin P, Moussalli J, Cadranel JF, Thibault V, Charlotte F, Dumouchel P, et al. Slow progression rate of fibrosis in hepatitis C virus patients with persistently normal alanine transaminase activity. Hepatology 1998;27:868–872.

[30] Ghany MG, Kleiner DE, Alter H, Doo E, Khokar F, Promrat K, et al. Progression of fibrosis in chronic hepatitis C. Gastroenterology 2003;124:97–104.

[31] Seidel N, Volkmann X, Langer F, Flemming P, Manns MP, Schulze-Osthoff K, et al. The extent of liver steatosis in chronic hepatitis C virus infection is mirrored by caspase activity in serum. Hepatology 2005;42:113–120.

[32] Shiffman ML, Hofmann CM, Contos MJ, Luketic VA, Sanyal AJ, Sterling RK, et al. A randomized, controlled trial of maintenance interferon therapy for patients with chronic hepatitis C virus and persistent viremia. Gastroenterology 1999;117:1164–1172.

[33] Omata M, Yoshida H, Toyota J, Tomita E, Nishiguchi S, Hayashi N, et al. A large-scale, multicentre, double-blind trial of ursodeoxycholic acid in patients with chronic hepatitis C. Gut 2007;56:1747–1753.

[34] Takano S, Ito Y, Yokosuka O, Ohto M, Uchiumi K, Hirota K, et al. A multicenter randomized controlled dose study of ursodeoxycholic acid for chronic hepatitis C. Hepatology 1994;20:558–564.

[35] Ortiz V, Berenguer M, Rayon JM, Carrasco D, Berenguer J. Contribution of obesity to hepatitis C-related fibrosis progression. Am J Gastroenterol 2002;97:2408–2414.

GASTROENTEROLOGY 2008;134:1396–1405

Potential Relevance of Cytoplasmic Viral Sensors and Related Regulators Involving Innate Immunity in Antiviral Response

YASUHIRO ASAHINA,* NAMIKI IZUMI,* ITSUKO HIRAYAMA,* TOMOHIRO TANAKA,* MITSUAKI SATO,*,‡ YUTAKA YASUI,* NOBUTOSHI KOMATSU,*,‡ NAOKI UMEDA,* TAKANORI HOSOKAWA,* KEN UEDA,* KAORU TSUCHIYA,* HIROYUKI NAKANISHI,* JUN ITAKURA,* MASAYUKI KUROSAKI,* NOBUYUKI ENOMOTO,‡ MEGUMI TASAKA,§ NAOYA SAKAMOTO,§ and SHOZO MIYAKE*

*Department of Gastroenterology and Hepatology, Musashino Red Cross Hospital, Tokyo; ‡First Department of Internal Medicine, Faculty of Medicine, University of Yamanashi, Yamanashi; and §Department of Gastroenterology and Hepatology, Tokyo Medical and Dental University, Tokyo, Japan

Background & Aims: **Clinical significance of molecules involving innate immunity in treatment response remains unclear. The aim is to elucidate the mechanisms underlying resistance to antiviral therapy and predictive usefulness of gene quantification in chronic hepatitis C (CH-C).** ***Methods:*** **We conducted a human study in 74 CH-C patients treated with pegylated interferon α-2b and ribavirin and 5 nonviral control patients. Expression of viral sensors, adaptor molecule, related ubiquitin E3-ligase, and modulators were quantified.** ***Results:*** **Hepatic RIG-I, MDA5, LGP2, ISG15, and USP18 in CH-C patients were up-regulated at 2- to 8-fold compared with non-hepatitis C virus patients with a relatively constitutive Cardif. Hepatic RIG-I, MDA5, and LGP2 were significantly up-regulated in nonvirologic responders (NVR) compared with transient (TR) or sustained virologic responders (SVR). Cardif and RNF125 were negatively correlated with RIG-I and significantly suppressed in NVR. Differences among clinical responses in RIG-I/Cardif and RIG-I/RNF125 ratios were conspicuous (NVR/TR/SVR = 1.3:0.6:0.4 and 2.3:1.3:0.8, respectively). Like viral sensors, ISG15 and USP18 were significantly up-regulated in NVR (4-fold and 2.3-fold, respectively). Multivariate and receiver operator characteristic analyses revealed higher RIG-I/Cardif ratio, ISG15, and USP18 predicted NVR. Lower Cardif in NVR was confirmed by its protein level in Western blot. Also, transcriptional responses in peripheral blood mononuclear cells to the therapy were rapid and strong except for Cardif in not only a positive (RIG-I, ISG15, and USP18) but also in a negative regulatory manner (RNF125).** ***Conclusions:*** **NVR may have adopted a different equilibrium in their innate immune response. High RIG-I/Cardif and RIG-I/RNF125 ratios and ISG15 and USP18 are useful in identifying NVR.**

Infection with hepatitis C virus (HCV) is a common cause of chronic hepatitis, which progresses to cirrhosis and hepatocellular carcinoma in many patients.[1] Although combination therapy with pegylated interferon (PEG-IFN) α and ribavirin is now established as the standard treatment for chronic HCV infection genotype 1b, the sustained virologic response rate in these patients is still around 50%.[2–4] Moreover, physicians have also found that 20% of patients are nonvirologic responders (NVR; those whose HCV-RNA does not become negative during 48 weeks of combination therapy).[5] Prediction of NVR status is of clinical importance because these patients have no chance of achieving a sustained virologic response even after prolonged combination therapy.[6] However, mechanisms involving resistance to PEG-IFN-α and ribavirin have not been fully elucidated, and it is difficult to predict treatment responses before initiation of PEG-IFN-α and ribavirin combination therapy.

In vitro studies have suggested that an innate immune response in viral infection is an essential part of the host antiviral defense system.[7] HCV evades the host immune response through a complex combination of processes that include signaling interference, effector modulation, and continual viral genetic variation.[8] We hypothesized that liver tissue would show a consistent difference between responders and nonresponders in expression levels of the gene involved in innate immunity and IFN signal transduction. These differences could be used to predict treatment outcomes.

The retinoic acid–inducible gene I (RIG-I), a cytoplasmic RNA helicase, and the related melanoma differentia-

Abbreviations used in this paper: CARD, Caspase-recruiting domain; Cardif, caspase-recruiting domain adaptor inducing IFN-β; G3PDH, glyceraldehyde-3-phosphate dehydrogenase; HCV, hepatitis C virus; IPS-1, IFN-β promoter stimulator I; ISG15, IFN-stimulated gene 15; PEG-IFN, pegylated interferon; MDA5, melanoma differentiation associated gene 5; MAVS, mitochondrial antiviral signaling protein; NVR, nonvirologic responders; PBMC, peripheral blood mononuclear cell; RIG-I, retinoic acid-inducible gene I; RNF125, ring-finger protein 125; ROC, receiver operator characteristic; SVR, sustained viral responder; TR, transient responder; UBP43, ubiquitin-specific protease 43; USP18, ubiquitin-specific protease 18; VISA, virus-induced signaling adaptor.

0016-5085/08/$34.00
doi:10.1053/j.gastro.2008.02.019

Table 1. Patient Characteristics at Baseline According to Final Virologic Response

	SVR n = 30	TR n = 24	NVR n = 20	*P* value
Age (*y*)	52 ± 13	60 ± 8.7	60 ± 10	.04[a]
Female % (M/F)	47% (16/14)	63% (9/15)	60% (8/12)	.5[b]
Naïve & Relapser[c]/Non-responder[c]	26/4	20/4	14/6	.3[b]
BMI	24.6 ± 3.0	24.9 ± 4.4	24.0 ± 2.1	.6[a]
ALT (*IU/L*)	75 ± 57	65 ± 35	68 ± 41	1.0[a]
Hemoglobin (*g/dL*)	14.3 ± 1.6	14.1 ± 1.1	14.5 ± 1.7	.6[a]
Platelet count ($\times 10^3/\mu L$)	182 ± 62	169 ± 48	140 ± 39	.04[a]
Liver histology				
A1/A2/A3	19/8/3	14/8/1	10/10/0	.3[b]
F1/F2/F3	14/9/7	11/7/5	7/5/8	.7[b]
Viral load ($\times 10^6$ *IU/mL*)	1.6 ± 1.2	1.8 ± 1.1	1.6 ± 1.1	.8[a]
Viral decline rate (log_{10}/day)				
First phase	2.1 ± 0.9	1.5 ± 0.6	0.7 ± 0.5	<.0001[a]
Second phase	0.05 ± 0.05	0.04 ± 0.02	0.006 ± 0.008	<.0001[a]

ALT, alanine aminotransferase; BMI, body mass index.
[a]*P* values were determined by Kruskal–Wallis test.
[b]*P* values were determined by chi-square test.
[c]Response to previous IFN treatment.

tion-associated gene 5 (MDA5) play essential roles in initiating the host antiviral response by detecting intracellular viral dsRNA.[9,10] Caspase-recruiting domain (CARD) adaptor inducing IFN-β (Cardif), also called IFN-β promoter stimulator 1 (IPS-1), mitochondrial antiviral signaling protein (MAVS), and virus-induced signaling adaptor (VISA), is an adaptor molecule. Cardif connects RIG-I sensing to downstream signaling, resulting in IFN-β gene activation.[11–14] On the other hand, RIG-I sensing has been shown to be negatively regulated in a dominant-negative manner by LGP2,[10,15] a helicase related to RIG-I and MDA5 lacking CARD. Interestingly, the ubiquitin ligase ring-finger protein 125 (RNF125) has been recently shown to conjugate ubiquitin to RIG-I, MDA5 as well as Cardif, which results in suppressing the functions of these proteins.[16] Furthermore, these molecules are conjugated (ISGylated) by IFN-stimulated gene 15 (ISG15), a ubiquitin-like protein,[17] and ISG15 is specifically removed from ISGylated protein by ubiquitin-specific protease 18 (USP18), also called ubiquitin-specific protease 43 (UBP43).[18,19] Moreover, the NS3/4A protease of HCV specifically cleaves Cardif as part of its immune evasion strategy.[11,20] Therefore, the RIG-I/Cardif system and its regulatory systems have essential key functions in the innate antiviral response (see Supplementary Figure 1 online at www.gastrojournal.org). However, the clinical significance of these innate immune systems, especially in relevance to the treatment response, is unclear because findings in this field have been mainly obtained by in vitro experiments using cell lines.

The aims of this study were to elucidate the mechanisms underlying resistance to antiviral therapy in the clinical setting and to determine whether quantification of transcripts of positive and negative cytoplasmic viral sensors and related regulatory molecules involving innate immune system is useful in predicting responses to PEG-IFN-α and ribavirin combination therapy.

Patients and Methods

Patients

Among patients with biopsy-proven chronic hepatitis C hospitalized at the Musashino Red Cross Hospital, 74 patients of HCV genotype 1b with a high viral load (>100,000 IU/mL by Amplicor-HCV Monitor Assay; Roche Molecular Diagnostics Co, Tokyo, Japan) were included in the present study (Table 1). Patients with cirrhosis, autoimmune hepatitis, or alcoholic liver injury were excluded. No patient was positive for hepatitis B virus–associated antigen/antibody or anti–human immunodeficiency virus antibody. No patient received immunomodulatory therapy prior to the enrollment. Written informed consent was obtained from all the patients, and this study was approved by the Ethical Committee of Musashino Red Cross Hospital in accordance with the Helsinki Declaration. Five patients with nonviral liver disease (2 had autoimmune hepatitis and 3 had primary biliary cirrhosis) were included in the present study as controls.

Treatment Protocol

The patients were treated for 48 weeks with subcutaneous injections of PEG-IFN-α-2b (PegIntron; Schering-Plough Corporation, Kenilworth, NJ) at a dose of 1.5 $\mu g \cdot kg^{-1} \cdot week^{-1}$. Ribavirin (Rebetol; Schering-Plough Corporation) was administered concomitantly over the 48-week period, given orally twice daily at a total daily dose of 600 mg for the patients who weighed less than 60 kg and 800 mg for the patients who weighed between 60 and 80 kg. The dose of PEG-IFN-α-2b was reduced to 0.75 $\mu g \cdot kg^{-1} \cdot week^{-1}$ when either the neutrophil count was $<750/mm^3$ or the platelet count was $<80 \times 10^3/mm^3$. The dose of ribavirin was reduced to 600 mg/day when the hemoglobin concentration decreased to <10 g/dL.